

T.C.
MUĞLA SITKI KOÇMAN UNIVERSITY
INSTITUTE OF NATURAL AND APPLIED SCIENCES

GEOLOGICAL ENGINEERING DEPARTMENT

LATE PLEISTOCENE-HOLOCENE CLIMATIC
CYCLES FROM LAKE VAN SEDIMENTS

MASTER OF SCIENCE THESIS

ZEKİ BORA ÖN

JUNE 2013
MUĞLA

T.C.
MUĞLA SITKI KOÇMAN UNIVERSITY
INSTITUTE OF NATURAL AND APPLIED SCIENCES

GEOLOGICAL ENGINEERING DEPARTMENT

**LATE PLEISTOCENE-HOLOCENE CLIMATIC
CYCLES FROM LAKE VAN SEDIMENTS**

MASTER OF SCIENCE

ZEKİ BORA ÖN

JUNE 2013

MUĞLA

MUGLA SITKI KOÇMAN ÜNİVERSİTESİ

Fen Bilimleri Enstitüsü

TEZ ONAYI

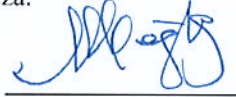
Zeki Bora Ön tarafından hazırlanan LATE PLEISTOCENE-HOLOCENE CLIMATIC CYCLES FROM LAKE VAN SEDIMENTS başlıklı tezinin, 06/06/2013 tarihinde aşağıdaki jüri tarafından Jeoloji Mühendisliği Anabilim Dalı'nda yüksek lisans derecesi için gerekli şartları sağladığı oybirliği/oyçokluğu ile kabul edilmiştir.

TEZ SINAV JURİSİ

Prof. Dr. Mehmet Namık Çağatay (Jüri Başkanı)

Jeoloji Mühendisliği Anabilim Dalı,
İstanbul Teknik Üniversitesi, İstanbul

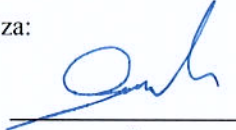
İmza:



Yrd. Doç. Dr. Murat Ersen Aksoy (Danışman)

Jeoloji Mühendisliği Anabilim Dalı,
Muğla Sıtkı Koçman Üniversitesi, Muğla

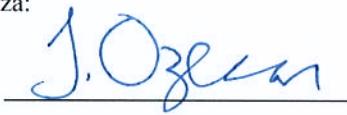
İmza:



Yrd. Doç. Dr. Mehmet Sinan Özeren (İkinci Danışman)

Jeoloji Mühendisliği Anabilim Dalı,
İstanbul Teknik Üniversitesi, İstanbul

İmza:



Doç. Dr. Murat Gül (Üye)

Jeoloji Mühendisliği Anabilim Dalı,
Muğla Sıtkı Koçman Üniversitesi, Muğla

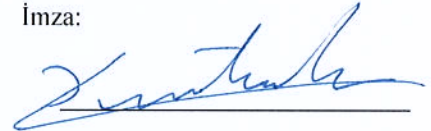
İmza:



Yrd. Doç. Dr. Bedri Kurtuluş (Üye)

Jeoloji Mühendisliği Anabilim Dalı,
Muğla Sıtkı Koçman Üniversitesi, Muğla

İmza:

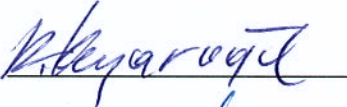


ANA BİLİM DALI BAŞKANLIĞI ONAYI

Prof. Dr. Fikret Kaçaroğlu

Jeoloji Mühendisliği Anabilim Dalı Başkanı,
Muğla Sıtkı Koçman Üniversitesi, Muğla

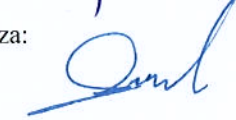
İmza:



Yrd. Doç. Dr. Murat Ersen Aksoy

Danışman, Jeoloji Mühendisliği Anabilim Dalı,
Muğla Sıtkı Koçman Üniversitesi, Muğla

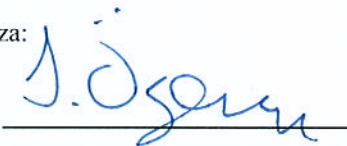
İmza:



Yrd. Doç. Dr. Mehmet Sinan Özeren

İkinci danışman, Jeoloji Mühendisliği Anabilim Dalı,
İstanbul Teknik Üniversitesi, İstanbul

İmza:



Savunma Tarihi: 06/06/2013

I hereby declare that all information in this document has been obtained and presented in accordance with academic rules and ethical conduct. I also declare that, as required by these rules and conduct, I have fully cited and referenced all material and results that are not original to this work.

Zeki Bora Ön

06/06/2013.



ABSTRACT
**LATE PLEISTOCENE-HOLOCENE CLIMATIC CYCLES FROM LAKE
VAN SEDIMENTS**

Zeki Bora ÖN

Master of Science (M.Sc.)

Institute of Natural and Applied Sciences

Department of Geological Engineering

Supervisor: Asst. Prof. Dr. Murat Ersen AKSOY

Co-supervisor: Asst. Prof. Dr. Mehmet Sinan Özeren

June 2013, 75 pages

Search for periodicity in the climatic records has been a matter of interest among the scientists since Joseph Adhemar. For this study, we have looked for the global and possible regional climate cycles within Lake Van ICDP sediment cores.

Borehole undisturbed sediment cores reaching to a composite depth of 145.5 were recovered in 2010 from 245 m water depth in the Northern Basin of Lake Van, within framework of International Scientific Continental Drilling Programme (ICDP). The cores were sampled and analysed by İTU-EMCOL team for project work funded by TÜBİTAK. The team carried out the core analyses. The geochronological analysis with the age model for the drilled sequence reveals the record extends back to 90400 years at the base of the sequence.

The geochemical results obtained by the XRF Core Scanner (X-ray Fluorescence) method for elemental analyses and mass spectrometric method for stable isotope analyses in total carbonate were subjected to Fourier transform after filtering and detrending. Since the time dimension of the data is unevenly spaced we chose the method of Lomb-Scargle Periodogram, which is an application of Fast Fourier Transform, and used it to search for the periodicities.

The results of the analyses of the longest climate records so far obtained from Anatolia show the presence of the precession cycle (21 ka), harmonics of the Milankovitch cycles (16.7, 12.3, 10.65, 9, 5.8, 4.25, 3.6 and 2.6 ka), Dansgaard/Oeschger and Bond cycles (1500 years), 1200 year periodicity, solar cycles (200, 86 and 22 years) and 125, 65, 41, 33 year periodicities in the data sets.

Keywords: Lake Van, Late Pleistocene, Periodicity, Climate cycles, Paleoclimate

ÖZET
VAN GÖLÜ ÇÖKELLERİNDE GEÇ PLEYİSTOSEN-HOLOSEN
İKLİM KAYITLARININ DÖNGÜSELLİĞİ

Zeki Bora ÖN

Yüksek Lisans Tezi

Fen Bilimleri Enstitüsü

Jeoloji Mühendisliği Anabilim Dalı

Danışman: Yrd. Doç. Dr. Murat Ersen AKSOY

İkinci Danışman: Yrd. Doç. Dr. Mehmet Sinan ÖZEREN

Haziran 2013, 75 sayfa

Periyodik iklim döngülerinin (örneğin Milankoviç döngüleri) araştırılması, özellikle Joseph Adhemar'dan bu yana, bilim insanları arasında ilgi uyandıran bir konu olmuştur. Bu çalışmada küresel kabul edilen ve muhtemel yerel iklim döngüleri Van Gölü ICDP çökel karotlarında araştırılmıştır.

Uluslararası Kıtasal Sondaj Programı (ICDP) ile 2010 yılında Van Gölü Kuzey Havzasında 245 m su derinliğinden 145,5 m uzunluğunda bozulmamış karot alınmıştır. TÜBİTAK tarafından desteklenen bir proje ile bu karotlar İTÜ-EMCOL ekibi tarafından örneklenmiştir. Aynı ekip alınan karotlarda izotop, XRF ve toplam organik/inorganik karbon analizi yapılmış ve stratigrafik istifin yaş modelini elde etmiştir. Bu çalışmalara göre incelenen sondajın stratigrafik kesitinin yaşı 90400 yıl öncesine değin uzanmaktadır.

X-ışınları Floresans (XRF) yöntemi ile elde edilen element analiz sonuçları ile toplam karbonattan elde edilen duraylı oksijen ve karbon izotopu analiz sonuçları; bu çalışmada zaman serileri olarak ele alınıp veriler filtrelenip detrend edildikten sonra sonuçlarda Fourier dönüşümü ile döngüsellik aranmıştır. Veriler zaman boyutunda eşit aralıklarla dağılmadığı için yöntem olarak, Hızlı Fourier Dönüşümünün bir uygulaması olan, Lomb-Scargle Periyodogram spektral metodu seçilmiştir.

Anadolu coğrafyasında ilk kez bu uzunlukta elde edilen veri setlerinin döngüsellik analizleri, Van Gölü çökellerinde Milankoviç döngülerinden olan ekinoksların deviniminin (21 ka), Milankoviç döngülerinin harmoniklerinin (16.7, 12.3, 10.65, 9, 5.8, 4.25, 3.6 and 2.6 ka), Dansgarrd/Oeschger ve Bond döngülerinin (1500 yıl), 1200 yıllık bir döngünün, solar döngülerin (200, 86 ve 22 yıl), ve 125, 65, 41, 33 yıllık döngülerin varlığını göstermektedir.

Anahtar Kelimeler: Van Gölü, Geç Pleistosen, Döngüsellik, İklim Döngüleri

To my lovely wife, who showed me to see the Gaia in a different manner

FOREWORD

My advisors Dr. M. Sinan Özeren and Dr. M. Ersen Aksoy will never be forgotten with their help and support.

Within this study the most appreciated help was from my lovely wife Dr. Sena Akçer. She convinced me to study Earth sciences and she was involved within all steps of this thesis.

Prof. Dr. M. Namık Çağatay shared his ongoing project and the data of the projects, namely PaleoVan ICDP and TÜBİTAK “Van Gölü'nün Geç Pleyistosen-Holosendeki Yüksek Çözünürlüklü Su Seviyesi Salınımları”, without any hesitation. Thanks for all his help. Furthermore I would like to thank to Emre Damcı, Dr. Ümmühan S. Sancar, Dr. Demet Biltekin, Nazik Öğretmen, Dursun Acar and all the İTÜ-EMCOL team.

Prof. Dr. A.M. Celal Şengör, Prof. Dr. Mehmet Sakınç, Dr. Cengiz Zabcı and Prof. Dr. Ahmet Hamdi Kayran encouraged me through my education and through the thesis, thanks for their invaluable support.

I would like to thank Assoc. Prof. Dr. Murat Gül for the times that we had brain stormings. My roommates Taner Korkmaz and M. Erde Bilir gave me the most innovative ideas during the cold winter and the hot Muğla summer.

And my parents Fadime Ön and İ. Halil Ön, without them I was nothing but a mineral in the soil. My grandmother and my sister must be thanked for their encouraging conversations with me.

TABLE OF CONTENTS

ABSTRACT	iv
ÖZET	v
FOREWORD	vii
TABLE OF CONTENTS	viii
LIST OF TABLES	x
LIST OF FIGURES	xi
LIST OF ABBREVIATIONS	xiv
1. INTRODUCTION	1
1.1. Historical Perspective	1
1.2. Studies on Climate Cycles around Lake Van Region	5
1.3. Aim and Scope	6
1.4. Study Area	8
1.4.1. Geography of the region.....	8
1.4.2. Geology of the region.....	8
1.4.1. Paleoclimate and today’s climate of the region	10
2. MATERIALS AND METHODOLOGY	18
2.1. Materials and Analytical Methods	18
2.1.1. Cores	18
2.1.2. Itrax X-Ray fluorescence (XRF) core scanner.....	18
2.1.3. Total organic (TOC) and total inorganic carbon (TIC) analyses	19
2.1.4. Stable isotope analyses.....	20
2.1.5. AMS radiocarbon dating	20
2.1.6. Age model	20
2.2. Methodology of Spectral Analysis	22
2.2.1. Simple moving average.....	22
2.2.2. Detrending.....	22
2.2.3. Spectral analysis.....	23

2.2.3.1. <i>Periodogram</i>	23
2.2.3.2. <i>The normalized Lomb-Scargle Periodogram</i>	24
2.2.3.3. <i>Probability distribution of the Lomb-Scargle Periodogram</i>	27
3. RESULTS AND DISCUSSION	28
3.1. Results	28
3.1.1. Spectral analysis results of 0-90.4 ka interval.....	29
3.1.2. Spectral analysis results of 0-13.5 ka interval.....	31
3.1.3. Spectral analysis results of 0-1 ka interval.....	34
3.2. Discussion	36
4. CONCLUSIONS	43
BIBLIOGRAPHY	45
APPENDICES	64
CURRICULUM VITAE	76

LIST OF TABLES

Table 1.1. Main rivers flowing to Lake Van (Çiftçi et al., 2008)	8
Table 3.1 Statistically significant spectral peaks (ka) gathered by LSP analysis for the 0-90.4 ka interval in Van5034_1 records. The significance level is chosen to be 95%. “*” denotes the arithmetic mean of two close values mentioned in the results section. B’s on the first column represent the bands.	37
Table 3.2 Theoretical periods of GLT which correlate with our results.....	38
Table 3.3 Worldwide spectral examples of some previous studies, correlating with our results, numbers are represented in ka. In the uppermost row given numbers represent the references in the following order: (1) Pestiaux et al., 1988, (2) Yiou et al., 1991, (3) Hagelberg et al., 1994, (4) Yiou et al., 1994, (5) Mommersteeg et al., 1995, (6) Mayewski et al., 1997, (7) Ortiz et al., 1999, (8) Wara et al., 2000, (9) Kloosterboer-van Hove et al., 2006, (10) Weber et al., 2010.	38
Table 3.4 Statistically significant spectral peaks (ka) gathered by LSP analysis for the 0-13.5 ka interval in Van5034_1 records. The significance level is chosen to be 95%. “*” shows the values chosen between 80 and 95% significance level.....	39
Table 3.5 Statistically significant spectral peaks (ka) gathered by LSP analysis for the 0-1 ka interval in Van5034_1 records. The significance level is chosen to be 95%.	42

LIST OF FIGURES

Fig. 1.1 Drainage basin of Lake Van (NB represents the location of the sediment core drilled at northern basin).....	7
Fig. 1.2 Simplified geological map of the Lake Van region. (Mutlu et al, 2012).....	10
Fig. 1.3 The high resolution of North Greenland Ice Core Project (Andersen et al., 2004) oxygen isotope record that spans the last 123,000 years. H1 to H6 are the Heinrich events and the numbers up to 25 are the documented Dansgaard/Oeschger events (Clement and Peterson, 2008).	12
Fig. 1.4. Mean positions of the main circulation systems affecting the region, namely Polar Front Jet (PFJ), Subtropical Jet (STJ), Intertropical Convergent Zone (ITCZ), and the pressure systems affecting the region, namely Continental Polar Air Mass (cP), Marine Polar Air Mass (mP), Continental Tropical Air Mass (cT), Marine Tropical Air Mass (mT) (Litt et al., 2009; modified from Wigley and Farmer, 1982).	14
Fig. 1.5. The differences between the negative and positive modes of NAO (Hoerling et al., 2010).	15
Fig. 1.6. Anomaly circulation of NCP a) during its negative phase, b) during its positive phase (Kutiel and Benarorch, 2002).	15
Fig. 1.7. An example of the laminated sediments of Lake Van. The black layer shows a tephra layer (Litt et al., 2009).	17
Fig. 2.1. Bathymetric map of Lake Van. NB (Northern Basin) and AR (Ahlat Ridge) show the locations of the core drilling sites (Stockhecke et al., 2012).	19
Fig. 2.2. Age model based on tephra ages, AMS ¹⁴ C ages, varve counting and isotopes (Çağatay et al., 2013).....	21
Fig. 3.1. Normalized LSP of the δ ¹⁸ O data, filtered by simple moving average over three consecutive samples, spanning the last 90400 years. The average	

interval of the data is 315 years. The dashed line shows 95% confidence level.....	29
Fig. 3.2. . Normalized LSP of the $\delta^{13}\text{C}$ data, filtered by simple moving average over three consecutive samples, spanning the last 90400 years. The average interval of the data is 315 years. The dashed line shows 95% confidence level.....	30
Fig. 3.3. Normalized LSP of the TOC data, filtered by simple moving average over three consecutive samples, spanning the last 90400 years. The average interval of the data is 315 years. The dashed line shows 95% confidence level.....	30
Fig. 3.4. Normalized LSP of the TIC data, filtered by simple moving average over three consecutive samples, spanning the last 90400 years. The average interval of the data is 315 years. The dashed line shows 95% confidence level.....	31
Fig. 3.5. Normalized LSP of the Ca/Ti data, spanning the last 13500 years, filtered by simple moving average over fifty consecutive samples and sampled one sample from every fifty consecutive data, making the average sample interval 19 years. The dashed line shows 95% confidence level.	32
Fig. 3.6. Normalized LSP of the Sr/Ca data, spanning the last 13500 years, filtered by simple moving average over fifty consecutive samples and sampled one sample from every fifty consecutive data, making the average sample interval 19 years. The dashed line shows 95% confidence level.	33
Fig. 3.7. Normalized LSP of the Mn/Ti data, spanning the last 13500 years, filtered by simple moving average over fifty consecutive samples and sampled one sample from every fifty consecutive data, making the average sample interval 19 years. The upper and lower dashed lines show 95% and 80% confidence level respectively.	33
Fig. 3.8. Normalized LSP of the Fe data, spanning the last 13500 years, filtered by simple moving average over fifty consecutive samples and sampled one sample from every fifty consecutive data, making the average sample interval 19 years. The dashed line shows 95% confidence level.	34

Fig. 3.9. Normalized LSP of the Ca/Ti data, spanning the last 1000 years, filtered by simple moving average over four consecutive samples and sampled one sample from every four consecutive data, making the average sample interval 1.25 years. The dashed line shows 95% confidence level. 35

Fig. 3.10. Normalized LSP of the Sr/Ca data, spanning the last 1000 years, filtered by simple moving average over four consecutive samples and sampled one sample from every four consecutive data, making the average sample interval 1.25 years. The dashed line shows 95% confidence level. 35

Fig. 3.11. Normalized LSP of the Mn/Ti data, spanning the last 1000 years, filtered by simple moving average over four consecutive samples and sampled one sample from every four consecutive data, making the average sample interval 1.25 years. The dashed line shows 95% confidence level. 36

Fig. 3.12. Normalized LSP of the Fe data, spanning the last 1000 years, filtered by simple moving average over four consecutive samples and sampled one sample from every four consecutive data, making the average sample interval 1.25 years. The dashed line shows 95% confidence level. 36

Fig. 3.13 Locations of the previous studies (Table 4.2). The numbers written on the map are a representative of the numbers in front of the names in the Table 4.2. “*” is an indicator of several core samples drilled near the same location. 41

LIST OF ABBREVIATIONS

$\delta^{13}\text{C}$	Delta 13 Stable Carbon Isotope Fractionation
$\delta^{18}\text{O}$	Delta 18 Stable Oxygen Isotope Fractionation
a.s.l.	Above Sea Level
AMS	Accelerator Mass Spectrometry
AR	Ahlat Ridge
BP	Before Present
EMCOL	Eastern Mediterranean Centre for Oceanography and Limnology
ICDP	International Continental Drilling Program
İTÜ	İstanbul Teknik Üniversitesi
ka	Kilo-annum
LSP	Lomb-Scargle Periodogram
Ma	Mega-annum
NAO	North Atlantic Oscillation
NB	Northern Basin
NCP	North Sea-Caspian Pattern
TC	Total Carbon
TIC	Total Inorganic Carbon
TOC	Total Organic Carbon
XRF	X-Ray Fluorescence

1. INTRODUCTION

1.1. Historical Perspective

Sir Norman Lockyer (1872) stated the following:

“Surely in meteorology, as in astronomy, the thing to hunt down is a cycle, and if that is not to be found in the temperate zone, then go to frigid zones, or the torrid zones and look for it, and if found, then above all things, and in whatever manner, lay hold of, study it, record it, and see what it means.”

The search for periodicity in the climatic records has been a matter of interest since the early nineteenth century. We, as humanity, try to understand the behaviour of the past climates and try to make projections onto future.

Before the 19th century, people had problems to explain the erratic boulders, moraines or polished rocks, which were mostly apart from their source rocks and they thought that these morphological features are the remains of a biblical flood. However, some scientists of the time chose to explain the erratics with the theory of glaciers like Hutton in 1795, Playfair in 1802, Venetz in 1821 and Esmark in 1827. James Hutton discussed the existence of the erratics and the u-shaped valleys, which he observed in the Jura while he was a medical student in Paris. John Playfair, a student and a close friend of Hutton, recognized that it was impossible that such boulders like weighing 2500 tons can move all the way over hills and valleys, separating from the source rock of them. So he thought that these boulders must have been transported by the immense power of the glaciers, that is to say, glaciers once covered these areas, which are now ice-free. But the valid explanations of Hutton and Playfair couldn't enlighten the society. In 1821 Ignace Venetz, a Swiss engineer, wrote a book about a climate change and according to him this was clearly observed by the moraines of the Alps (Hutton, 1795; Playfair, 1802; Venetz, 1821; Forbes, 1843; Seylaz, 1962; Davies, 1968; Andersen, 1992; Bard, 2004). Nearly at the same time, most probably, unaware of Venetz, Jens Esmark, a Norwegian geologist, had come to the similar results, yet he deduced the extension of ice cover was global. He

suggested that, in the formation of the solar system the Earth was a huge comet and its orbit's eccentricity (i.e. how much the orbit of the Earth around the Sun deviates from a circle, with the Sun located at one of the focal points of the resulting ellipse) was so great. Therefore the Earth enters an ice age at aphelion, leaves the ice age when it was at perihelion and this was a periodic behavior, so according to him the ice ages belonged to the formation of the Earth (Esmark, 1827; Andersen, 1992; Bard, 2004). While these hypotheses were being created, Jean de Charpentier insisted on the idea of ice age and made Louis Agassiz convince on the idea. Jean de Charpentier, stated that the geometry and the way of the standing on the ground of these blocks do not represent a horizontal, i.e. fluvial, transportation. Therefore to explain all these features, the appreciation of the glacier morphology and the extent of the glaciers were needed at the mid 19th century (de Charpentier, 1836, 1837; Bard, 2004). Louis Agassiz named the term "Ice Age" after the observations on Aar Glacier and according to him most of the northern Europe was covered by ice moreover he changed the name ice age to "Great Ice Age" after his observations in North America in 1846 (Agassiz, 1840; Summerfield, 1991; Bard, 2004; Turney, 2008).

After the ice age concept had come to life, Joseph Adhémar (1842) proposed that the ice age was not a single event. According to his hypothesis, glaciations must be periodic and controlled by the celestial mechanics (Bard, 2004). He concluded that, precession of the equinoxes is responsible for the insolation difference of the hemispheres and hence responsible for the ice ages. Precession of the equinoxes is the combination of the precession of the Earth's axis (which is presented by Hipparchus of Nicaea in about 130 B.C.) and precession of the Earth's orbit. According to him the northern and the southern hemispheres enter to an ice age regularly and after an interval of 10.5 ka the seasons will be reversed. Therefore, he correctly deduced the period of the precession of the equinoxes, which is approximately 21 ka (Allaby, 2004; Bard, 2004).

After the acceptance of ice age concept by the community, an astronomic cause for the ice ages wasn't that popular till James Croll's research. James Croll, in his early life, had almost no formal education and worked as a millwright, a house joiner, a tea merchant, a hotel manager and an insurance salesman. When he was 38 years old he

was hired as a janitor by the Glasgow Andersonian College and Museum in 1859 and he got the chance to spend time in the library (Oldroyd, 1996; Turney, 2008). In 1864 he published his first paper, “On the Physical Cause of the Climate Change During Geological Epochs”, and three years later two more papers showed up. According to him the ice ages are mainly controlled by celestial mechanics and there exists three parameters, which are namely: the precession of the equinoxes, the change in the obliquity of the Earth’s axis of rotation and the change of the Earth’s orbits eccentricity and the affect of these astronomical parameters have to cause alternating cold periods in both hemispheres, moreover his calculations showed that the last ice age began 240000 years before present and the last warm period lasted for 80000 years. He argued that the decrease in the sunlight received favors the accumulation of snow and the increase of the area covered by snow, hypothetically, would amplify the accumulation of snow, which is called positive feedback (Croll, 1864, 1867a, 1867b; Bard, 2004; Berger, 2012). With these assumptions Croll made a projection of the climate by taking account of the astronomical parameters, for three million years before present and for one million years after present (Croll, 1875). Croll’s ideas gained a serious popularity; also his ideas were argued in Charles Darwin’s book “*The Origin of Species*”, 6th edition (Darwin, 1872; Berger, 2012). In 1909 Penck and Brückner studied on the alluvial terraces observed around tributaries of Danube and they claimed the existence of four major glaciations, which they named Günz, Mindel, Riss and Würm, and these results seemed to support Croll’s multiple quasi-periodic glaciations theory (Penck and Brückner, 1909; Bard, 2004; Berger, 2012).

However serious criticisms began to blame Croll’s theory, depending on two bases. The first test was alternating glaciation of the two hemispheres idea seemed to be wrong. Geomorphological observations were pointing; the glaciations were synchronous in both hemispheres. Another test of the theory of Croll was made on his calculation of the duration of the present warm period. According to the observations the estimated duration seemed to be much shorter than 80000 years, as Croll suggested (Bard, 2004; Berger, 2012).

In 1941 Milutin Milankovitch, a Serbian civil engineer and an astronomer, took the idea of Croll and made the calculations in a much more mathematical fashion and

applied the theory on to the ideas of Penck and Brückner's four step glaciation. Furthermore he was the first to complete a full astronomical theory of Pleistocene ice ages in mathematical detail (Milankovitch, 1941; Berger, 1988; Grubic, 2006; Berger, 2012; Petrovic, 2012).

Milankovitch's theory of ice ages did not arouse interest until the work of Hays et al. (1976). Hays et al. (1976) showed for the first time that quasi-periods of 100, 41, 23 and 19 ka are present in the past climate records, and since then it has been studied by many researchers (Milankovitch, 1941; Imbrie, 1982; Berger, 1988; Berger, 2012 and references therein).

In 1981 Ghil and Le Treut proposes a new model which tries to understand the oscillations of the climate at higher frequencies, namely between $1/5$ and $1/15$ ka^{-1} . Their model is governed by three nonlinear equations that describe: (1) The evolution of the globally averaged temperature of the ocean-atmosphere system owing to changes in the radiation balance, (2) the evolution of polar ice caps owing to changes in precipitation budget and to motions of the underlying bedrock, and (3) the visco-elastic response of the crust and upper mantle to ice load variations (Kallen et al. 1979; Ghil and Le Treut, 1981; Le Treut and Ghil, 1983; Ghil and Childress, 1987; Le Treut et al., 1988). With these assumptions Le Treut et al. (1988) creates a simple isotopic model and calculates, by assuming the 41, 23 and 19 ka orbital periodicities as true astronomical ones, periodicities of 109, 14.7, 13, 11.5, 10.4 and 9.5 ka with spectral analysis, which are the harmonics of the orbital periodicities assumed.

The oxygen isotope data gathered from the ice cores show rapid oscillations during the Würm glacial (~115-10 ka BP) period, which give the characteristic sawtooth shape of the graphic of the data. Such events occurred 24 times that represent an abrupt warming phase in the glacial time. This cyclic behavior is called Dansgaard-Oeschger cycles and are thought to have a ~1500 year periodicity (Dansgaard et al., 1983; Dansgaard et al., 1984; Dansgaard et al., 1993; Mayewski et al., 1997; Alley et al., 2001; Ganopolski and Rahmstorf, 2002). These oscillations are thought to have been driven by salt oscillations in the North Atlantic (Broecker et al.,). A similar oscillation pattern, with ~1500 year periodicity, is claimed to occur in the Holocene and is called Bond cycles (Bond et al., 1997; Mayewski et al., 1997; Bianchi and

McCave, 1999; Bond et al., 1999; Bond et al., 2001; Wanner and Butikofer, 2008). A possible cause of this abrupt warming event depends on the changes in the thermohaline circulation of North Atlantic and the stochastic resonance behavior of the system or on solar variations (Bond et al., 1999; Alley et al., 2001; Bond et al., 2001).

Among the mentioned astronomical cycles the climate of the Earth has a strict bound to some other astronomic variations. The first one, Sun's variability which mainly controls the direct energy output of the Sun by ions streaming from Sun's spots that generate a magnetic field acting like a shield (Broecker, 2002; Gray et al., 2005). Solar variability is thought to be periodic and there are some numbers, which are accepted in the society. Among all, 11 year Schwabe and the harmonic of it 22 year Hale cycles are the most prominent ones (Sonett et al., 1997). Moreover the Gleissberg cycle (~80-90 year), the Suess cycle (~180-208 year), the Hallstattzeit cycle (~2400 year) and newly proposed ~6000 year cycle are thought to be periodicities of solar variations (Damon and Sonnet, 1991; Sonett et al., 1997; USGS, 2000; Vasiliev and Dergachev, 2002; Lean, 2005; Xapsos and Burke, 2009). The second variability is the lunar variability which is effective on tides and it is also thought to have effects on climate. It is called Saros Cycle and has a length of 18.6 year (Hoyt and Schatten).

1.2. Studies on Climate Cycles around Lake Van Region

Since the 19th century scientists have developed that climate of the Earth has its own periodic/quasi-periodic oscillations whereas that kind of studies are nearly absent in Turkey and in nearby geographies.

Rohling et al. (2002) found 2300 years of periodicities within the records of Aegean Sea cores covering the last 13 ka. Fleitmann et al. (2003) found 205, 132, 105, 90, 60 and 50 years of periodicities at the stalagmite records of Qunf cave in Oman, which span the last 10 ka. Prasad et al. (2004) searched for periodicities within the varve records of Lake Lisan (the Pleistocene lake, ancestor of the Dead Sea in Israel), which spans the interval between 26 – 17 ka BP. Lamy et al. (2006) found 800 and

500 years of periodicities within Black Sea and Red Sea core records. Jones et al. (2006) searched for the periodicities in Lake Nar core and found 135, 58 and 33 years of periodicity. Finally Fleitmann et al. (2009) studied the stalagmites of Sofular Cave in Zonguldak, Northwest Turkey, and they report that they found 500 years of periodicity within the records, which span the interval between 24 ka and 51 ka BP.

The studies, listed above, for Turkey implies that this geography needs more studies on the cyclic behavior of the climate/paleoclimate records. So one can ask if the cycles, which are thought to be global, did really affect Anatolia's past climate? Moreover, does Anatolia have its own system apart from the global cycles? We think, the results that are gathered within this study will be a representative of paleoclimate cycles (see Stockhecke et al. 2012), at least, for the Van region.

1.3. Aim and Scope

A 144 m undisturbed sediment core, which spans the last 90.4 ka, drilled at the northern basin of Lake Van (Fig. 1.1) by ICDP and the geochemical records gathered by İTÜ EMCOL scientists make it possible to search for the cycles in this sediment core data and try to understand the dynamics of the past climate of Lake Van region. This thesis looks for the cycles in the chemical records over time basis with the help of spectral methods. For that much long sediment core one can expect to see the following global climatic cycles:

1. The precession of the equinoxes cycle of the Milankovitch-Croll theory, which is approximately 21 ka.
2. The 1500 year cycle which is outlined by many researchers for the Late Pleistocene.
3. The solar cycles, namely Schwabe, Hale, Gleissberg, Suess, Hallstadtzeit.

Lake Van is a highly tectonically and volcanically active region. The region is on the border of Mediterranean climate and continental climate. Its sedimentation shows varve structures according to seasonal patterns (Landmann et al., 1996a; Stockhecke et al., 2012). Apart from the cycles mentioned above, the own oscillations of the

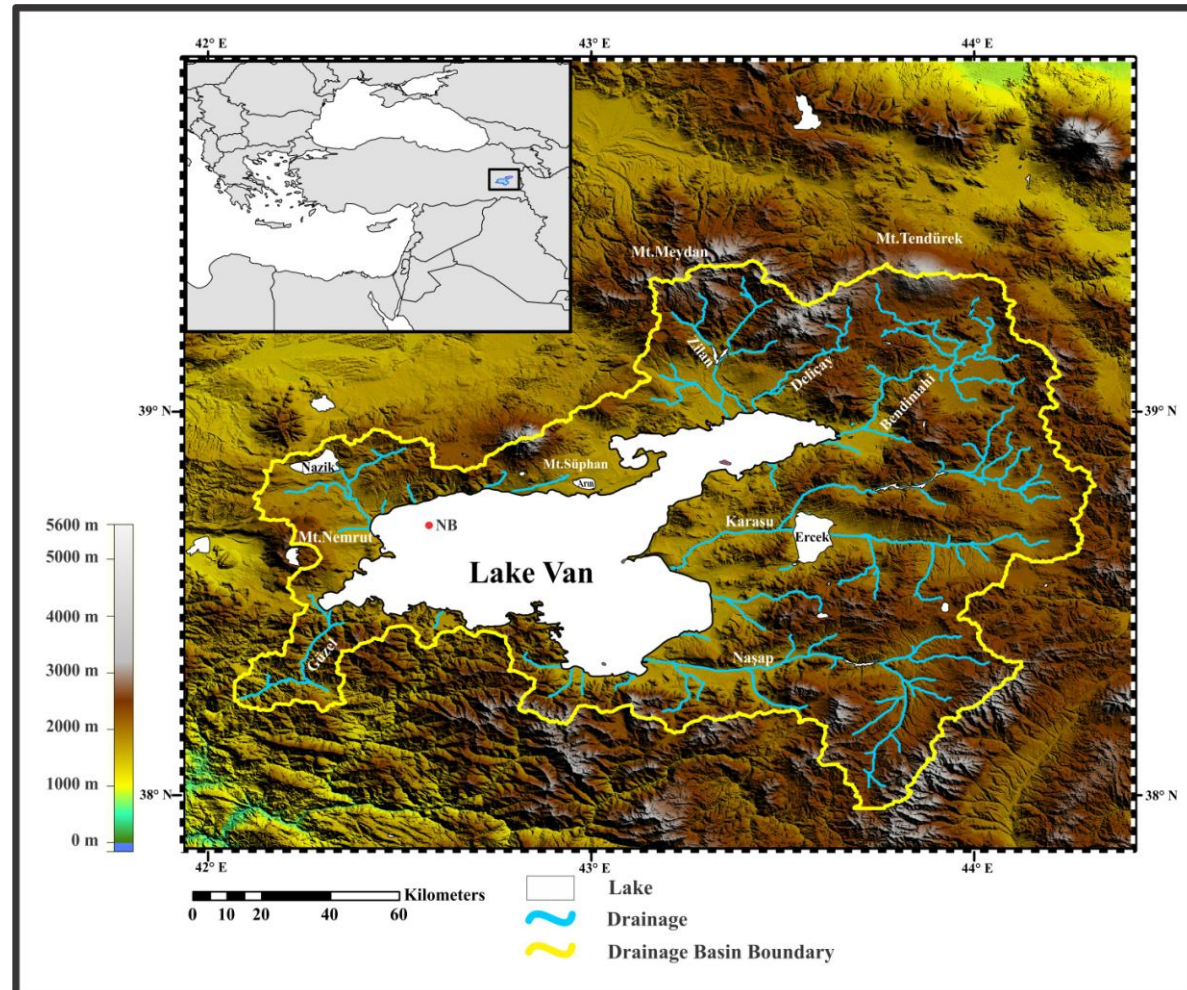


Fig. 1.1 Drainage basin of Lake Van (NB represents the location of the sediment core drilled at northern basin).

Lake Van region may exist and search for them may reveal the dynamical behavior of the lake and the regional climate.

1.4. Study Area

1.4.1. Geography of the region

Lake Van is the fourth largest closed lake and the largest alkaline lake of the world, which is surrounded by the Euphrates basin in the west, Tigris basin in the south and Arax basin in the east. The lake is on a high plateau located 1,650 m above sea level within the contractional province between the Eurasian and Afro-Arabian plates. The surface area of the lake is 3,602 km² and its drainage area covers 12,520 km². Today there are many small and large rivers draining into the lake (Table 1.1, Fig. 1.1).

Table 1.1. Main rivers flowing to Lake Van (Çiftçi et al., 2008)

Name of the river	Flow point	Length (km)
Zilan	Erciş	70
Bendimahi	Erciş	90
Deliçay	Erciş	55
Karasu	Van Merkez	148
Neşap	Gevaş	145
Memedik	Saray	60
Gevaş	Gevaş	14

The distribution of the bottom of the lake is as follows: 27% of the lake area has relatively shallow water and termed as lacustrine shelf, 63% of the area is the steeper lacustrine slope and 10% of the lake area is the deep flat plain. Flat plain, called Tatvan Basin, has 445 m average depth and its deepest point is recorded as 451 m (Kempe et al., 1978; Wong and Degens, 1978).

1.4.2. Geology of the region

The lake is a volcanic dammed lake, which originated according to Wong and Finckh (1978) at least 60 ka ago, according to Şaroğlu and Güner (1981) at the middle

Pleistocene, according to Çukur et al., (2013) ~550 ka ago, and was a part of the Zilan, Bendimahi and Murat river system. All the three publications state that, with the eruption of Nemrut volcano, during the constructional phase of Nemrut, the lava of the volcano dammed the ancient Murat Valley and consequently the lake formed. Lake Van-Muş Basin was separated into two sub-basins as a consequence of eruption of Nemrut Volcano (Şaroğlu and Güner, 1981).

Three tectonic units constitute the Eastern Anatolia high plateau, namely Eastern Rhodope-Pontide arc, Eastern Anatolian Accretionary Complex and Bitlis Pötürge Massif. The region's neotectonic evolution starts as shortening of Eastern Anatolia between the Arabian and Eurasian plates in the Middle Miocene, some more than 15 Ma ago. Tectonic forces generated east-west trending inclined folds and the region has become undulated. Moreover accompanying to tectonism, volcanism has caused variations on morphology such as asymmetry of folds, east-west trending vertical developed at the north-south borders of the basins, like Muş Basin. For now the basin faces strike-slip faulting rather than thrusting as a consequence of shortening (Şaroğlu and Güner, 1981; Dewey et al., 1986; Şengör et al., 2003; Şengör et al., 2008).

At the south of the lake the Southeastern Taurids is mainly composed of metamorphic units of the Paleozoic aged Bitlis Massif which is characterized by albite, albite-quartz, garnet micaceous schist, marble, phyllite, politic slate, recrystallized limestone, quartzite and radiolarites over a gneissic core. On the eastern side of the lake the Upper Cretaceous aged ultrabasics, flysch deposits, limestones and Oligocene aged conglomerates, sandstones, mudstones and limestones form the flatlands of the city of Van and its surroundings. On the northern and western shore there lie the Plio-Quaternary volcanic mountains and the eruptions create the units, which are basaltic, dacitic and andesitic rocks. There are four stratovolcanoes surrounding the lake. On the lake's western shore, Nemrut caldera stands 2948 m a.s.l., still active. According to Yılmaz et al. (1998) last eruption was in 1441 A.D. but Aydar et al. (2003) object this date and calls for the 1597 A.D. In the northwest Mount Süphan stands 4158 m a.s.l., inactive for the last 10,000 years. Meydan Volcano (3290 m a.s.l.) is at the north of the lake, and Tendürek Volcano, still active (3584 m a.s.l.) stands on the northeast of the lake. (Degens and Kurtman, 1978; Kurtman and Başkan, 1978; Degens et al., 1984; Kipfer et al., 1994; Yılmaz et al., 1998; Aydar et al., 2003; Keskin, 2003; Şengör et al., 2003; Şengör et al., 2008;

Kuzucuoğlu et al., 2010, Fig. 1.2).

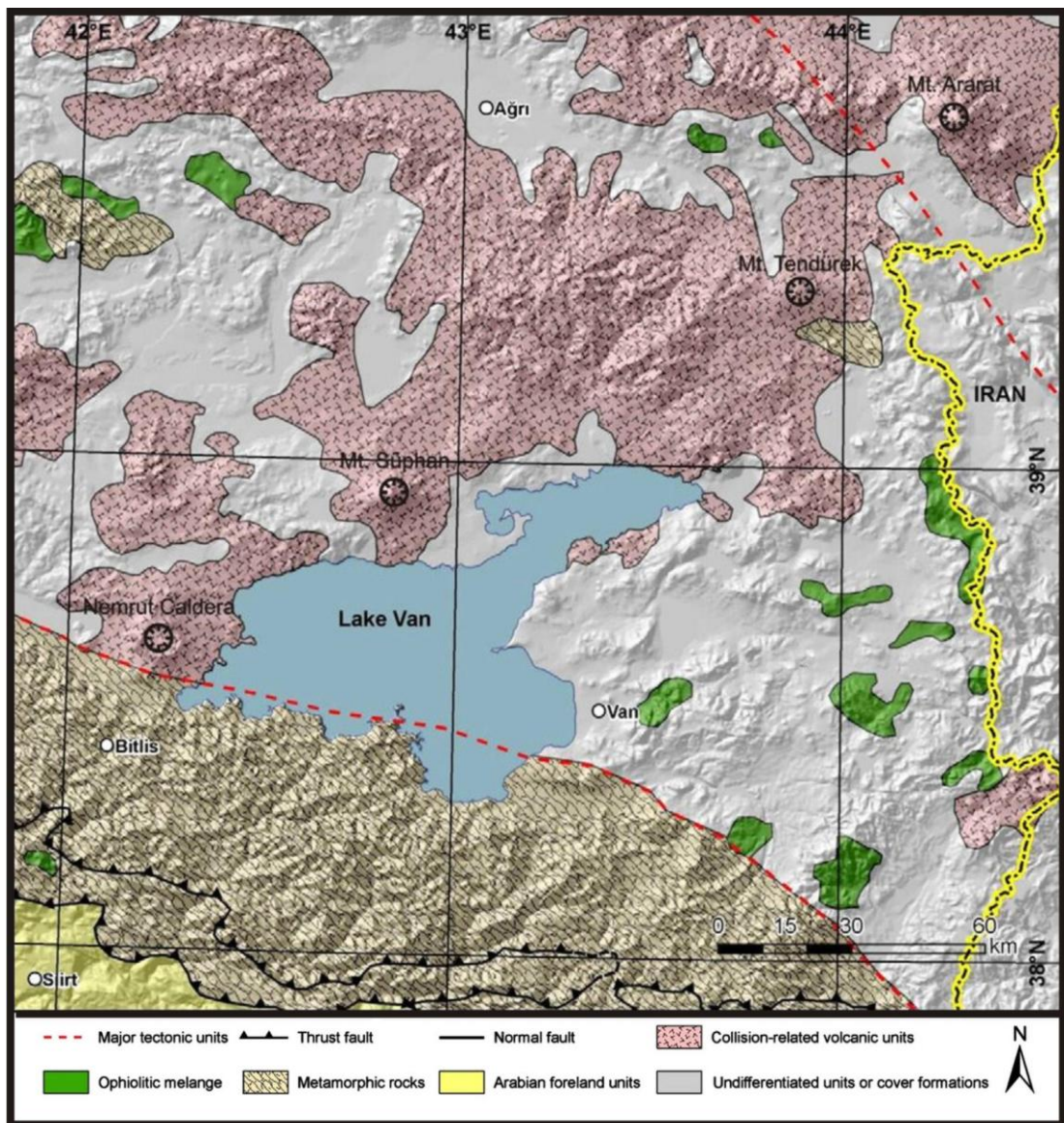


Fig. 1.2 Simplified geological map of the Lake Van region. (Mutlu et al, 2012).

1.4.1. Paleoclimate and today's climate of the region

To understand today's climate one should take a look at the Cenozoic cooling. Today still there are many debates about the causes of the ongoing cooling. There are some opinions about the cause (For a detailed summary see Denton, 1999; Zachos et al., 2001). After the Eocene Thermal Maximum (~51 Ma), when the deep sea temperatures were 12°C warmer than today (Savin et al., 1975), first ice caps in Antarctica began to form some 45.5 Ma ago (Ehrmann and Mackensen, 1992). After

this time a gradual cooling was on the way, but Tertiary is marked by three major cooling events. After a 17 Ma lasting of cooling trend a major temperature decline marks the boundary of Eocene and Oligocene, some 34 Ma ago, which caused the formation of Antarctic ice sheets. The second major decline of the temperatures is dated between 17 to 15 Ma ago at middle Miocene that formed permanent Antarctic ice sheets. Earth's climate faced the third decline at the start of Quaternary, 2.6 Ma ago (Miller et al., 1987; Denton, 1999; Zachos et al., 2001). Quaternary Period was the time of glacials and interglacials, which occurred quasi-periodically. The interval of 2.52-0.95 Ma was dominated by the obliquity bandwidth of 41 ka and after 0.95 Ma the 100 ka frequency took the control of the climate oscillations (Denton, 1999).

The last interglaciation, namely Eemian, had its warmest period, which at that time was warmer than today and had smaller or equal to today's ice volume, around 122 ka BP (CLIMAP Project Members et al., 1984). The temperatures fell by more than 2°C in the deep oceanic waters after 122 ka BP (Broecker and Denton, 1990; Denton, 1999). For the last glacial, the times of massive discharges of icebergs into the North Atlantic, that are observed as ice-rafted detritus in marine cores, are called Heinrich events and six of them are defined for the last 60 ka BP (Heinrich, 1988; Bard et al., 2000; Hemming, 2004, Fig. 1.3). The timing of Heinrich events coincides well with the fluctuations of the ice core data observations (Bond et al., 1993). According to these data Heinrich events are cold periods followed by warm intervals. After the detailed $\delta^{18}\text{O}$ values gathered from the Greenland ice cores it was observed that the climate was highly irregular during the last glaciation and the abrupt transitions of the climate from a colder phase (stadial) to a warmer phase (interstadial) are called Dansgaard/Oeschger cycles (Dansgaard et al., 1983; Dansgaard et al., 1984). Last glaciation reached its maximum around 20 ka BP. The temperatures and the amount of atmospheric greenhouse gases began to increase until 14.5 ka BP, after that time Earth faced a cold spell, namely Younger Dryas, from 12.7 ka until 11.7 ka BP (Cuffey and Clow, 1997; Clark et al., 2012). Bard et al. (2000) call the Younger Dryas event as a Heinrich event and named it as H0. The warm period Holocene, which is rather stable than Würm, starts 11.7 ka BP (Gradstein et al., 2012).

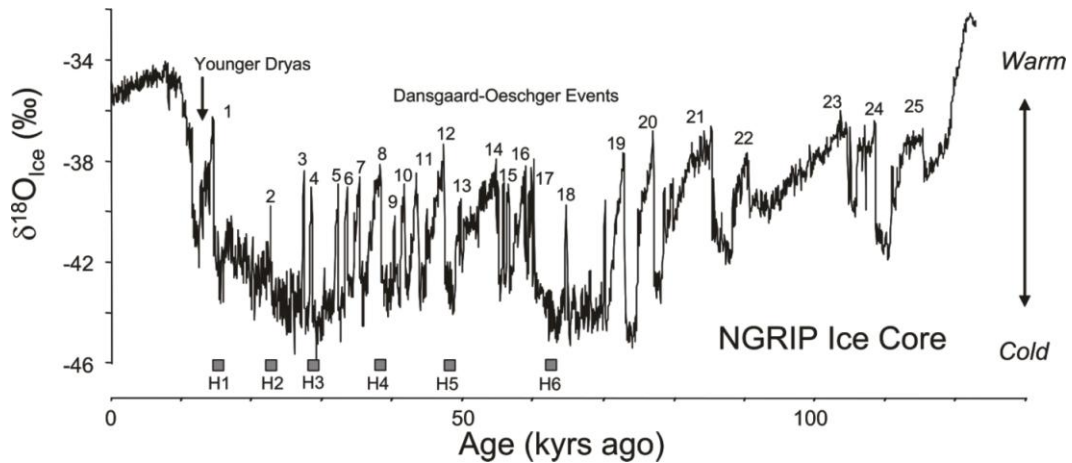


Fig. 1.3 The high resolution of North Greenland Ice Core Project (Andersen et al., 2004) oxygen isotope record that spans the last 123,000 years. H1 to H6 are the Heinrich events and the numbers up to 25 are the documented Dansgaard/Oeschger events (Clement and Peterson, 2008).

During the last glaciation, Lake Van had experienced lake level fluctuations, which left terraces as proofs around the lake. Kuzucuoğlu et al. (2010) have found four transgression series, first of them dated back to 115 ka BP and the second of them is dated back to 100 ka BP. According to Kuzucuoğlu et al. (2010) the first transgression may be the result of either volcanism or tectonic events but the second transgression is associated with the relative warm or moist period of the region between 100 ka BP and 35 ka BP. The next two transgressions are dated to 26 ka BP and 20 ka BP, which are moist times of Eastern Mediterranean (Roberts and Wright, 1993; Öğretmen, 2012). After that time a regression of the lake is documented in the varves of the lake. Around 15 ka BP the lake has completely dried according to Landman et al. (1996b) but the study of Northern Basin composite core by Öğretmen (2012) shows that the level of the lake has dramatically dropped but the whole lake didn't dry. After 14.6 ka BP lake level rose and had a regression around 9 ka BP and this regression coincides with Caucasian and Central Asian low lake levels which is in contrast with the Indo-Arabian lakes (Roberts and Wright, 1993; Landmann et al., 1996b). During the Holocene, lake level rose up to its highest-level around 7.5 ka BP and dropped to today's level around 3 ka BP (Landmann et al., 1996b). Moreover, unlike Western Anatolia the occurrence of the advance of the forests in Holocene is relatively late. At sites close to the sea, in Turkey, the forestation was complete around 9 ka BP whereas in Van region yet it was not complete 6 ka BP and among this period steppe-fire frequency was high. Both suggest dry spring and summer

during the early Holocene (Roberts and Wright, 1993; Wick et al., 2003). Around 4 ka BP the region's climate reached today's wetter conditions (Degens et al., 1984; Wick et al., 2003; Öğretmen, 2012).

Climate systems cannot be explained by monotonic concepts; moreover the climate of the eastern Mediterranean is complex enough and has not been yet fully understood (Akçar and Schlüchter, 2005).

Anatolia's weather is under the control of marine and continental tropical air masses and marine and continental polar air masses (Fig. 1.4). These systems are controlled by movements of subtropical and subpolar high pressure systems through north and south according to seasons. With the movement of the subtropical high pressure system to the north the region experiences drier conditions. In winter, the subtropical high pressure system moves southward and the region gets under the effect of Siberian high pressure system and the polar and continental air masses take the control of the region (Harding et al., 2009).

North Atlantic Oscillation (NAO) is mostly responsible for the climate of Europe, Mediterranean and North Africa (Hurrell, 1995; Visbeck et al., 2001; Visbeck, 2002; Harding et al., 2009). Station-based index of NAO is defined as the the sea surface pressure differences between two stations, one lie in subpolar and the other lie in subtropical regions of North Atlantic, which are Stykkisholmur/Iceland and Ponta Delgada/Azores (Rogers, 1997) or Stykkisholmur/Iceland and Lisbon/Portugal (Hurrell, 1995) or Reykjavik and Gibraltar (Jones et al., 1997). In the so-called positive mode of NAO, which is the sea level pressure below normal over Iceland and above normal over Azores, Europe faces stronger than average westerlies, USA faces more southerly flows than average and the Canadian Arctic, west Greenland and the Mediterranean faces anomalous northerly flows. In the negative mode of NAO, which is relative higher pressure over Iceland and relative lower pressure over Azores, creates colder air on Europe and USA and a stormy weather over Mediterranean in winters (Hurrell et al., 2001; Wallace and Hobbs, 2006, Fig. 1.5). According to Cullen and deMenocal (2000), Anatolia is the easternmost limit of NAO and in the positive mode of NAO colder and drier conditions persist in Anatolia. For example, northern Syria retains NAO signals but much weaker than

Turkey and they find no significant correlation in Iraq. Furthermore they claim that Tigris streamflows and especially Euphrates streamflows are associated with NAO.

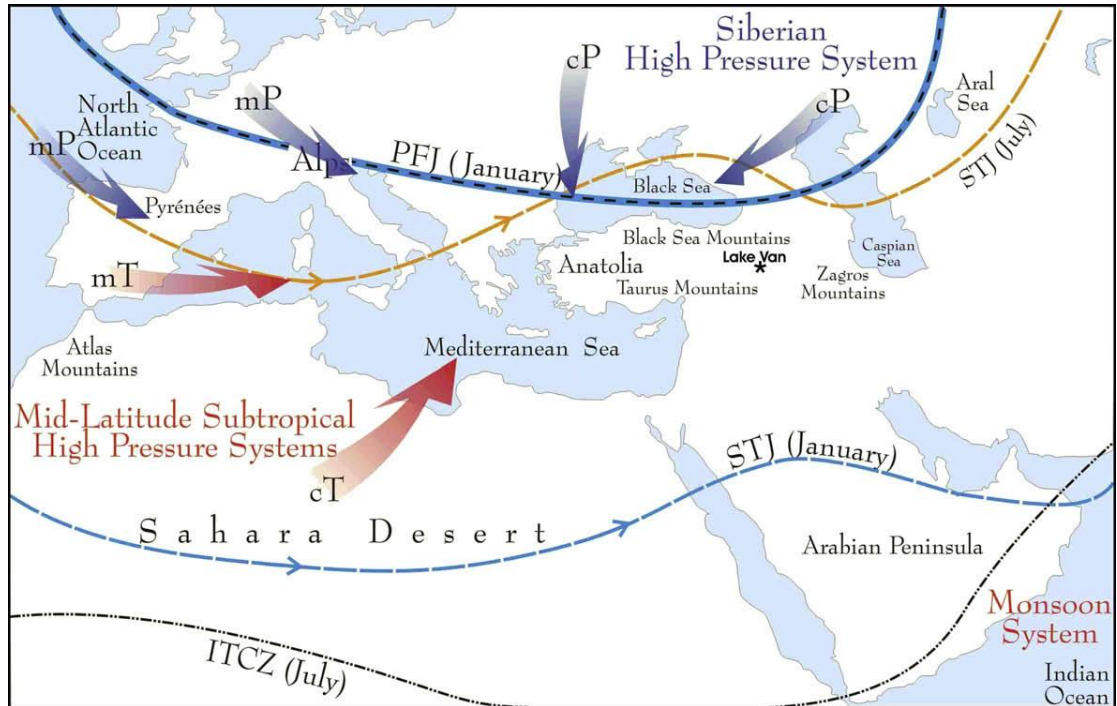


Fig. 1.4. Mean positions of the main circulation systems affecting the region, namely Polar Front Jet (PFJ), Subtropical Jet (STJ), Intertropical Convergent Zone (ITCZ), and the pressure systems affecting the region, namely Continental Polar Air Mass (cP), Marine Polar Air Mass (mP), Continental Tropical Air Mass (cT), Marine Tropical Air Mass (mT) (Litt et al., 2009; modified from Wigley and Farmer, 1982).

Kutiel and Benarorch (2002) defined an oscillation system that is effective on Eastern Mediterranean. They named it as North Sea-Caspian Pattern (NCP). NCP is calculated by taking the difference of geopotential heights at upper level atmospheric values over the North Sea and Caspian Sea. According to them, the negative index of NCP brings an increased southwesterly anomaly circulation towards the Balkans, western Turkey and the Middle East and higher temperatures plus aridity is observed, whereas positive index brings northwesterly circulation towards the Black Sea and creates colder conditions than the normal conditions (Kutiel and Benarorch, 2002; Kutiel et al., 2002; Göktürk, 2005; Gündüz and Özsoy, 2005; Kutiel and Türkeş, 2005, Fig. 1.6).

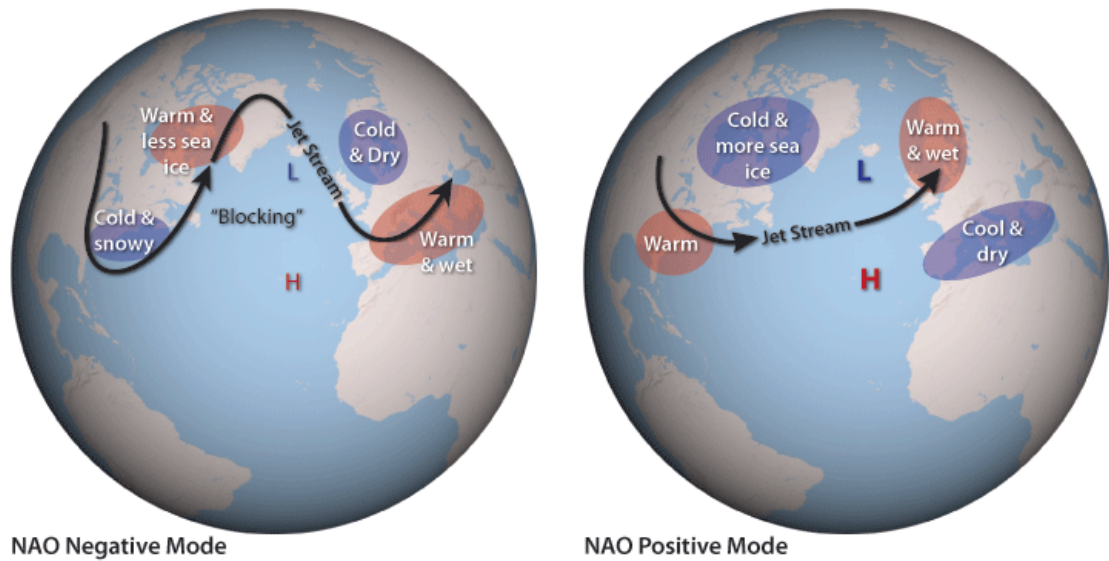


Fig. 1.5. The differences between the negative and positive modes of NAO (Hoerling et al., 2010).

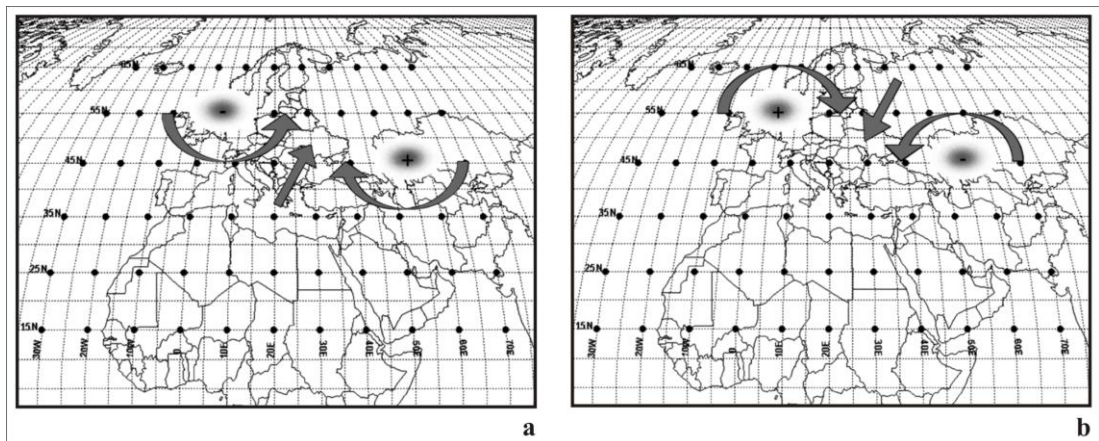


Fig. 1.6. Anomaly circulation of NAO a) during its negative phase, b) during its positive phase (Kutiel and Benarorch, 2002).

Lake Van region experiences continental climate, according to Köppen-Geiger climate classification it falls into Ds climate type, i.e. it is mainly a humid, cold mid latitude climate but has dry summers (Peel et al., 2007, Türkeş, 2010). Monthly average temperatures are below 0°C between December and February and around 20°C during summer, long term monthly average temperature is 9.2°C (Turkish State Meteorological Service, 2013). Annual precipitation is around between 380-700 mm (Elkatmış, 2008). The eastern Mediterranean's climate differs from the western Mediterranean climate by its dryness and larger temperature differences between

summer and winter (Harding et al., 2009). Erol (2011) calls the eastern Mediterranean's climate as continental Mediterranean. As the region precipitation mostly shows up itself at the end of the spring and at the beginning of summer, according to Erol (2011), that situation is called Late Mediterranean Precipitation Regime. This shows that the region lies in a transition zone between Mediterranean winter precipitation regime and mid latitude continental summer regime. According to Ünal et al. (2003) the region is climatically on the border of southeastern Anatolian region and eastern Anatolian region. Yet, the occurrence of the oro-mediterranean type forest on the southwest of the lake and the steppe type forests on the north and east is another indicator of the region being a transitional climatic zone (Roberts and Wright, 1993).

Annually the lake loses 4.2 km^3 of water by evaporation, balances it by surface runoff of 1.7 km^3 , and by precipitation of 2.5 km^3 (Kempe et al., 1978). Lake level fluctuations has been recorded since 1944 and according to Kempe et al. (1978) the correlation of the solar activity and the lake level fluctuations is visible to eye with a clear periodicity. Between 1944 and 1970 the lake level fluctuates regular and periodic (Kempe et al., 1978), however for the period of 1985-1995 the level rose significantly and Kadioğlu et al. (1995) claim that these fluctuations are closely related to meteorological phenomena. Therefore this shows that, as a closed lake, Lake Van is sensible to climatic/meteorological changes.

Stockhecke et al. (2012) report that the annual particle cycle of the lake is suitable for varve formation which can be used to study past climates. According to their study, the sedimentation is controlled by seasonal patterns. Higher particle fluxes are observed in spring by precipitation and snowmelt. In winter nearly no flux is observed but in summer carbonate flux is high and according to the study these conditions are ideal for varve formation and so paleoclimate studies (Landmann et al., 1996a; Stockhecke et al. 2012, Fig. 1.7). Moreover dust storms must be effective for the summer fluxes which must also be considered as a sediment parameter (Huguet et al., 2012).

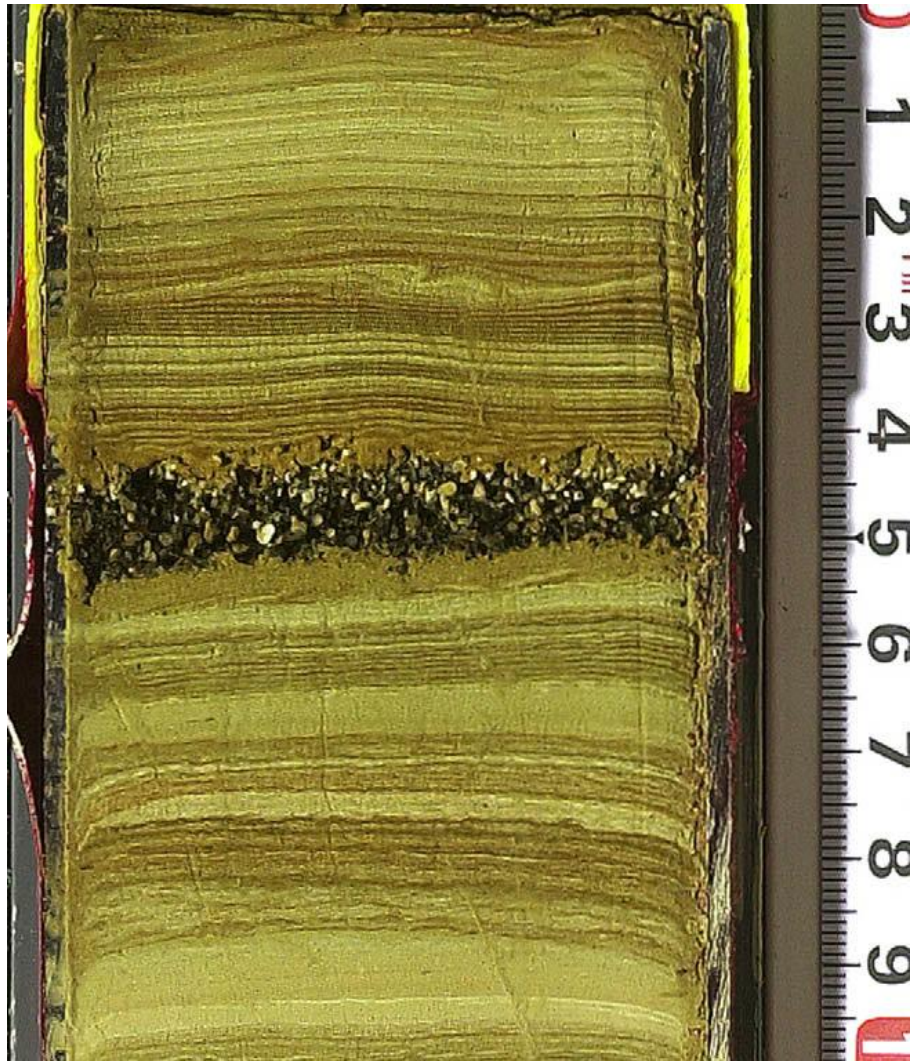


Fig. 1.7. An example of the laminated sediments of Lake Van. The black layer shows a tephra layer (Litt et al., 2009).

2. MATERIALS AND METHODOLOGY

For this thesis we have used the chemical data of the 144 m long composite sediment core of Paleovan project carried out by International Continental Drilling Programme (ICDP) (see Litt et al., 2012) from the Northern Basin of Lake Van. İTÜ EMCOL scientists carried out lithological description and sampling of the cores. They established a composite stratigraphic section and age model for the site and studied the lake level changes using multi-proxy analyses, such as XRF core scanner and stable isotope analyses, and varve counting (Öğretmen, 2012; Çağatay et al., 2013).

2.1. Materials and Analytical Methods

This thesis uses the data generated by the İTÜ EMCOL team during the course of a TÜBİTAK project entitled “High resolution water level changes of Lake Van during Pleistocene-Holocene” (Çağatay et al., 2013)

2.1.1. Cores

In the framework of Paleovan project during summer 2010 the ICDP Expedition 5034 retrieved 144 m long undisturbed sediment cores, named Van5034_1, at the site called Northern Basin (NB) which is 5 km offshore from Ahlat, 245 m below lake level at 38.7051 N latitude and 42.568 E longitude (Fig. 2.1).

2.1.2. Itrax X-Ray fluorescence (XRF) core scanner

Itrax Core Scanner provides high-resolution optical and radiographic images and elemental profiles of sediment cores. This instrument consist of a central measuring tower incorporating an X-Ray focusing unit and a range of sensors which are optical-line camera, laser topographic scanner, X-Ray line camera for measuring the transmitted X-Rays and high count rate XRF detection system. It is optional to scan entire length of samples from 1 centimeter to 200 μ m.

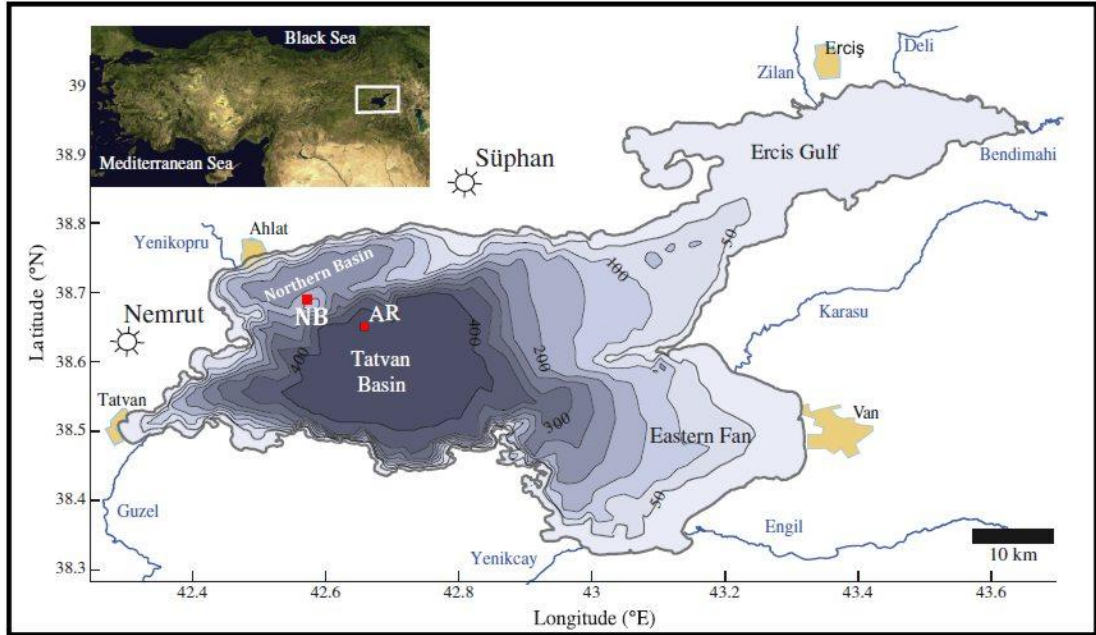


Fig. 2.1. Bathymetric map of Lake Van. NB (Northern Basin) and AR (Ahlat Ridge) show the locations of the core drilling sites (Stockhecke et al., 2012).

The Northern Basin core from Lake Van was analyzed, in İTÜ EMCOL laboratories, with 500 μ m step-size, counting for 10 seconds, and optical image resolution is 50 μ m pixel⁻¹ for sediment cores. XRF Core Scanner analyzed the following elements' intensity: Al, Si, P, S, Cl, Ar, K, Ca, Sc, Ti, V, Cr, Mn, Fe, Co, Ni, Cu, Zn, Ga, Ge, As, Se, Br, Rb, Sr, Y, Zr, Nb, Mo, Cd, Sb, I, Cs, Ba, La, Ce, Hf, Ta, Pb, Th, U.

2.1.3. Total organic (TOC) and total inorganic carbon (TIC) analyses

TOC/TIC analyses are performed in İTÜ EMCOL laboratories by EMCOL scientists with Shimadzu TOC/TIC Analyzer. The samples of 50-100 mg, which have been pounded in an agate mortar after dried at 60°C, have been analyzed to calculate the total carbon (TC) and TIC percentage and TOC percentage is calculated by subtracting the TIC percentage from the TC percentage.

The analysis of sample's TC calculation mainly depends on the analyzer's detection of CO₂ gaseous amount while burning the samples at 900°C. To calculate the amount of TIC, after adding 85% phosphoric acid to the sample, the sample is heated at 200°C. Within this process the amount of the CO₂ gaseous is detected by the

analyzer to estimate the TIC percentage. These analyses have the precision of better than 2% at 95% confidence level (for details, see Çağatay et al., 2013).

2.1.4. Stable isotope analyses

$\delta^{18}\text{O}$ and $\delta^{13}\text{C}$ analyses are performed from the bulk carbonate of the laminated sediment samples in Environmental Geochemistry Laboratory at University of Arizona by using mass spectrometry. For the stable isotope measurements, this device establishes a precision down to 0.02% (Becker and Dietze, 2000; Becker, 2002).

2.1.5. AMS radiocarbon dating

Three samples of plant remains are sent to University of Arizona, Environmental Geochemistry Laboratory and Accelerator Mass Spectrometry is used to date these samples. After the AMS ^{14}C dating is established the ages are converted to calendar year using IntCal option of Calib 6.1 computer software (Reimer et al., 2004).

2.1.6. Age model

İTÜ EMCOL scientists established the age model by AMS ^{14}C analysis, varve counting, Marine Isotope Stage correlations and tephra layer correlations. The tephra layers, dated by varve counting by Landman (1996), Landmann et al. (1996a, 1996b), Çağatay et al. (2013) and dated by $^{40}\text{Ar}/^{39}\text{Ar}$ dating method by Sumita and Schminke (2013), are correlated with the Marine Isotope Stages. These data are then correlated with the core records and by using AnalySeries software the data are converted to the age model (Fig. 2.2).

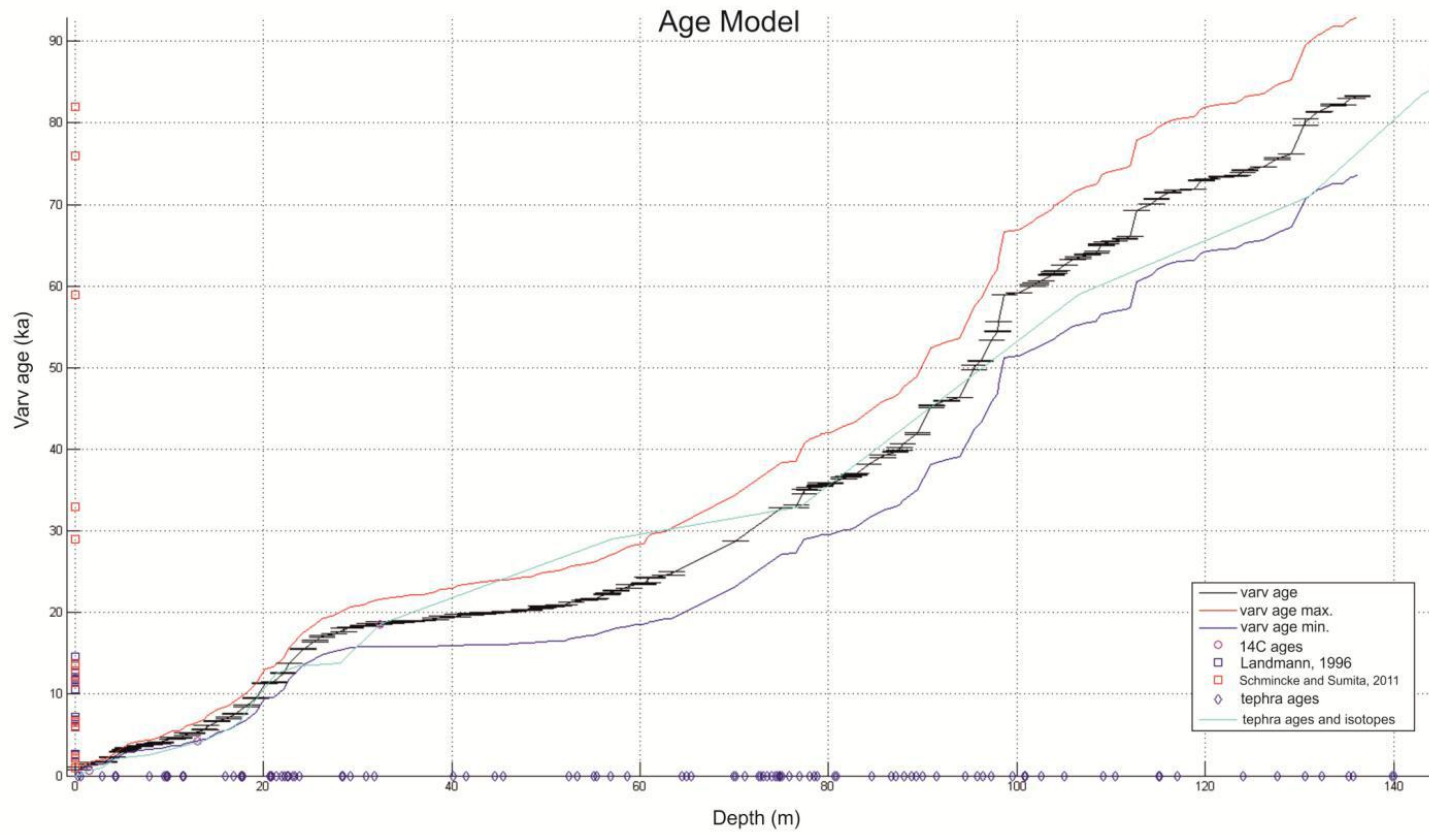


Fig. 2.2. Age model based on tephra ages, AMS ^{14}C ages, varve counting and isotopes (Çağatay et al., 2013)

2.2. Methodology of Spectral Analysis

All the calculations mentioned in this section are performed on MATLAB software.

2.2.1. Simple moving average

Natural time series are generally accepted as a combination of the signal and noise. To separate these two, generally linear filters are used to smooth the series (Bloomfield, 2000). Simple moving average, explained below, is the method to filter the time series that we have used in this thesis.

Suppose we have a time series $h(t)$ such that

$$h_k = h(t_k), k = 0, 1 \dots N - 1. \quad (2.1)$$

Generally mathematical representation of the filtering process is called the convolution and represented by;

$$h_f(t) = \sum_{m=-N_1}^{N_2} [c_m \cdot h(t - m)], \quad (2.2)$$

where N_1 and N_2 are positive integers and N_1+N_2 is called the order of the filter and c_m is the vector of filter weights. If one chooses $N_1=N_2$, say N , and c_m as a constant, say c , that is;

$$c = \frac{1}{2N + 1}, \quad (2.3)$$

then the filter is called the simple moving averaging (Chatfield, 1996; Bloomfield, 2000; Trauth, 2010). Whenever the window exceeds the data for the boundary values, to avoid the loss of information, we preferred to calculate the average for the values that fall inside the window.

2.2.2. Detrending

In the long-term climate time series might have a trend, e.g. Cenozoic cooling trend after Eocene thermal maximum (Denton, 1999). This trend can cause a small pseudo-

frequency show up in the calculations and is better to remove this trend (Muller and MacDonald, 2000). In this thesis we have detrended the series by subtracting the arithmetic mean of the series from the data vector.

2.2.3. Spectral analysis

2.2.3.1. Periodogram

To search for periodicities in time series, Fourier Transform method and its applications are essential. Periodogram is the simplest way of finding the frequencies of series.

Suppose we have a data set of equally spaced in time with N elements. Let the discrete data set be defined as follows;

$$h_k = h(t_k), t_k = k\Delta t, k = 0, 1 \dots N - 1. \quad (2.4)$$

In the equation (2.4) h represents for the values of the data in time and Δt represents the difference between consecutive time elements. Since a transformation of a data set having N elements cannot have outputs more than N elements, with the Nyquist frequency principle, probable frequencies will lie in the closed interval;

$$\left[-\frac{1}{2\Delta t}, \frac{1}{2\Delta t}\right] \quad (2.5)$$

and the frequencies can be found at the values;

$$f_n = \frac{n}{N\Delta t}, n = -\frac{N}{2} \dots \frac{N}{2}. \quad (2.6)$$

If we draw an analogy between the continuous and discrete Fourier transforms, we get;

$$\begin{aligned} H(f_n) &= \int_{-\infty}^{\infty} h_t e^{2\pi i f_n t} dt \approx \sum_{k=0}^{N-1} h_k e^{2\pi i f_n t_k} \Delta t \\ &= \Delta t \sum_{k=0}^{N-1} h_k e^{2\pi i k n / N}. \end{aligned} \quad (2.7)$$

The final summation in (2.7) is called the discrete Fourier transform of the N points h_k (Press et al., 2007). The spectral power P of the frequencies is calculated as follows;

$$P(f_n) = |H(f_n)|^2 / (N\Delta t). \quad (2.8)$$

2.2.3.2. *The normalized Lomb-Scargle Periodogram*

The main difference of the Lomb-Scargle Periodogram (LSP) from the “classical” periodogram is that for a given time series of unequally spaced data set, you don’t have to interpolate the data, which most of the time results in loss of information (Scargle, 1982).

Suppose we have N data points that are unequally spaced in time and let these data points to be defined as;

$$h_k = h(t_k), k = 0, 1 \dots N - 1. \quad (2.9)$$

The mean and the variance of the h_k ’s are defined as

$$\bar{h} = \frac{1}{N} \sum_{k=0}^{N-1} h_k \quad (2.10)$$

and

$$\sigma^2 = \frac{1}{N-1} \sum_{k=0}^{N-1} (h_k - \bar{h})^2 \quad (2.11)$$

Instead of evaluating the data on a per-time interval basis, by defining the τ given below, LSP evaluates the data on a per-point basis (Press et al., 2007);

$$\tan(4\pi f\tau) = \frac{\sum_{k=0}^{N-1} \sin 4\pi f t_k}{\sum_{k=0}^{N-1} \cos 4\pi f t_k} \quad (2.12)$$

and the normalized LSP, spectral power as a function of f, is defined for each frequency f by (Lomb, 1976; Scargle, 1982);

$$P(2\pi f) = \frac{1}{2\sigma^2} \left\{ \frac{[\sum_{k=0}^{N-1} (h_k - \bar{h}) \cos(2\pi f(t_k - \tau))]^2}{[\sum_{k=0}^{N-1} \cos^2(2\pi f(t_k - \tau))]} + \frac{[\sum_{k=0}^{N-1} (h_k - \bar{h}) \sin(2\pi f(t_k - \tau))]^2}{[\sum_{k=0}^{N-1} \sin^2(2\pi f(t_k - \tau))]} \right\}. \quad (2.13)$$

But it is obvious that the algorithm above is rather slow and it takes time to make the calculations. Therefore in this thesis we have used the algorithm presented by Press and Rybicki (1989), namely fast computation of the LSP.

Let

$$S_h = \sum_{k=0}^{N-1} (h_k - \bar{h}) \sin(2\pi f t_k), \quad (2.14)$$

$$C_h = \sum_{k=0}^{N-1} (h_k - \bar{h}) \cos(2\pi f t_k) \quad (2.15)$$

and

$$S_2 = \sum_{k=0}^{N-1} \sin 4\pi f t_k, \quad (2.16)$$

$$C_2 = \sum_{k=0}^{N-1} \cos 4\pi f t_k, \quad (2.17)$$

then by trigonometric addition/subtraction theorems and cosine double angle formula we can rearrange the following as;

$$\begin{aligned} \sum_{k=0}^{N-1} (h_k - \bar{h}) \cos(2\pi f(t_k - \tau)) \\ = C_h \cos(2\pi f \tau) + S_h \sin(2\pi f \tau), \end{aligned} \quad (2.18)$$

$$\begin{aligned} \sum_{k=0}^{N-1} (h_k - \bar{h}) \sin(2\pi f(t_k - \tau)) \\ = S_h \cos(2\pi f\tau) - C_h \sin(2\pi f\tau), \end{aligned} \quad (2.19)$$

$$\begin{aligned} \sum_{k=0}^{N-1} \cos^2(2\pi f(t_k - \tau)) \\ = \frac{N}{2} + \frac{1}{2} C_2 \cos(4\pi f\tau) + \frac{1}{2} S_2 \sin(4\pi f\tau), \end{aligned} \quad (2.20)$$

$$\begin{aligned} \sum_{k=0}^{N-1} \sin^2(2\pi f(t_k - \tau)) \\ = \frac{N}{2} - \frac{1}{2} C_2 \cos(4\pi f\tau) - \frac{1}{2} S_2 \sin(4\pi f\tau). \end{aligned} \quad (2.21)$$

Since t_k 's are not evenly spaced S_h , C_h , S_2 and C_2 cannot be calculated by Fast Fourier Transform. Press and Rybicki (1989) define a new method, which they call as extirpolation or reverse interpolation. Extirpolation provides evenly spaced data from given unevenly spaced data with the help of Lagrange interpolation by replacing the function value at an arbitrary point by several function values on a regular mesh such that sums over the mesh are a good approximation to sums over the original arbitrary point. Suppose that the function $h(t)$, known at unevenly spaced discrete points defined as;

$$h(t_i) = h_i \quad (2.22)$$

and $g(t)$ is a function which can be evaluated anywhere. Let \hat{t}_k be a sequence of evenly spaced points on a regular mesh then $g(t)$ can be approximated by Lagrange interpolation as

$$g(t) \approx \sum_k w_k(t) g(\hat{t}_k) \quad (2.23)$$

where the $w_k(t)$ are Lagrange polynomial interpolation weights (see for details Press et al., 2007). And the extirpolation process is as follows;

$$\begin{aligned}
\sum_{j=0}^{N-1} h_j g(t_j) &\approx \sum_{j=0}^{N-1} h_j \left[\sum_k w_k(t_j) g(\hat{t}_k) \right] \\
&= \sum_k \left[\sum_{j=0}^{N-1} h_j w_k(t_j) \right] g(\hat{t}_k) \equiv \sum_k \hat{h}_k g(\hat{t}_k)
\end{aligned} \tag{2.24}$$

where

$$\hat{h}_k \equiv \sum_{j=0}^{N-1} h_j w_k(t_j) \tag{2.25}$$

So (2.14), (2.15), (2.16) and (2.17) can be calculated by Fast Fourier Transforms, by replacing the required vectors gathered by (2.24) instead of h_j and $g(t_j)$ and then the calculations of (2.18), (2.19), (2.20) and (2.21) are straightforward (Press and Rybicki, 1989).

2.2.3.3. *Probability distribution of the Lomb-Scargle Periodogram*

Scargle (1982) states that the normalized LSP obeys the exponential distribution and Horne and Baliunas (1986) empirically show that, for a value of chosen M , the statistical significance level of the peaks can be calculated for the level z chosen as;

$$P(> z) = 1 - (1 - e^{-z})^M \tag{2.26}$$

Within this thesis we have chosen the value of M as equal to the length of the series and the length of the frequency sequence as equal to the twice of the length of the series (Press et al., 2007).

3. RESULTS AND DISCUSSION

3.1. Results

We have investigated the periodicity of the records of the Van5034_1 core data with the help of the methods described in the previous section. These calculations, in fact, pick the sinusoidal frequencies, which lie in the geochemical data of the cores and the frequencies found are interpreted as paleoclimate cycle signals.

We have discussed the data in three sections; firstly, for all the data spanning the 90400 years, secondly for the data spanning the last 13500 years and lastly for the data spanning the last 1000 years. For the first part $\delta^{18}\text{O}$, $\delta^{13}\text{C}$, TIC and TOC data were used. We couldn't use the XRF data for that period since the data's resolution was not suitable to gather meaningful results; it had gaps and the accumulations of the data were scattered. Therefore XRF data were chosen to analyze the last 13500 years, because the scattering of the accumulation of the data was high and among all, the Holocene cycles may give interesting results for today's climate. And lastly the data were analyzed for the last 1000 years to check for short periods. And also, the stable isotope and organic/inorganic carbon data's resolutions were not suitable to reevaluate for shorter periods, since the data did not have sufficiently high resolution.

The reader should read the plots below as the horizontal axis representing the frequency component with the year^{-1} unit and the vertical axis representing the relative power component of the distinct frequency values.

For some disciplines, like, economics or remote sensing engineering, the value of the power of a frequency has meanings but for paleoclimate data the power of a frequency is only a relative indicator among all the frequencies in a plot (Muller and MacDonald, 2000).

3.1.1. Spectral analysis results of 0-90.4 ka interval

For all the data, spanning the last ~90 ka, we preferred the simple moving average of order three. The statistically significant, over 95% confidence level, periods are listed below.

Oxygen isotope data is a good proxy to determine the temperatures at which the geological formations were laid down and for closed lakes, it is assumed to be relative humidity/aridity and, especially in closed lakes, evaporation/precipitation indicator (Urey, 1947; Emiliani, 1955; Wick et al., 2003; Gat, 2010). Spectral analysis of stable oxygen isotope ($\delta^{18}\text{O}$) data gives periodicities of 33000, 21300, 12500, 10650, 9050, 4700 and 1375 years (Fig. 3.1).

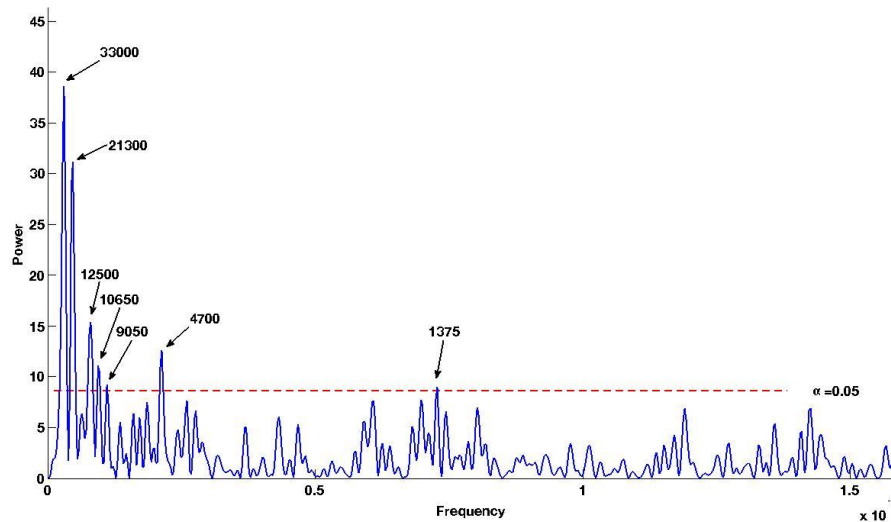


Fig. 3.1. Normalized LSP of the $\delta^{18}\text{O}$ data, filtered by simple moving average over three consecutive samples, spanning the last 90400 years. The average interval of the data is 315 years. The dashed line shows 95% confidence level.

In closed lakes Carbon isotope data is covariant with oxygen isotope data, but in hyper-alkaline lakes this assumption may fail. But it is sensitive to the organic productivity and the volume changes of the closed lakes (Talbot, 1990; Li and Ku, 1997; Leng et al., 2006, Roberts et al., 2008). Spectral analysis of stable carbon isotope ($\delta^{13}\text{C}$) data gives periodicities of 33000, 21000, 16500, 12500, 10300, 5750, 4150, 1375 and 640 years (Fig. 3.2).

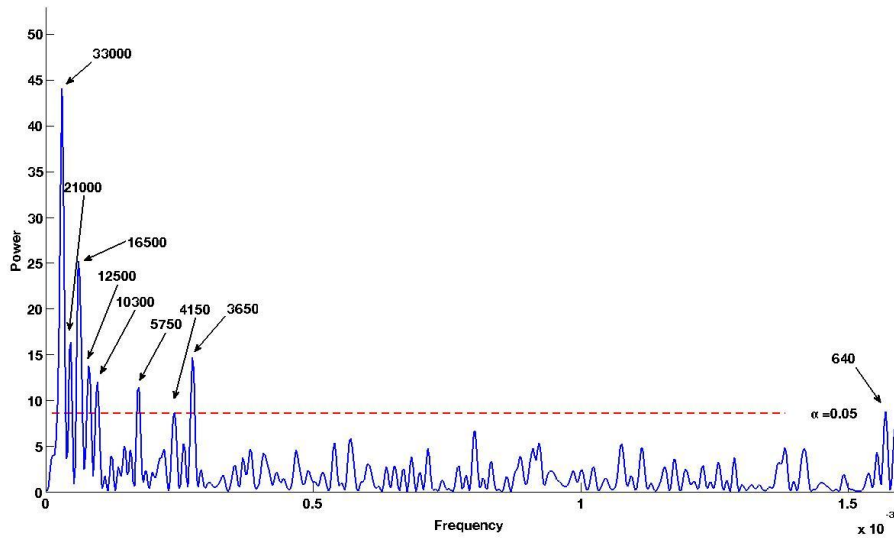


Fig. 3.2. . Normalized LSP of the $\delta^{13}\text{C}$ data, filtered by simple moving average over three consecutive samples, spanning the last 90400 years. The average interval of the data is 315 years. The dashed line shows 95% confidence level.

TOC is a representative of organic productivity in the lake (Meyers, 1997; Budziak et al., 2000, Cohen, 2003) Spectral analysis of TOC data gives periodicities of 36000, 22600, 17200, 12500, 11000, 5830, 3900, 3650, 3500 and 2600 years (Fig. 3.3).

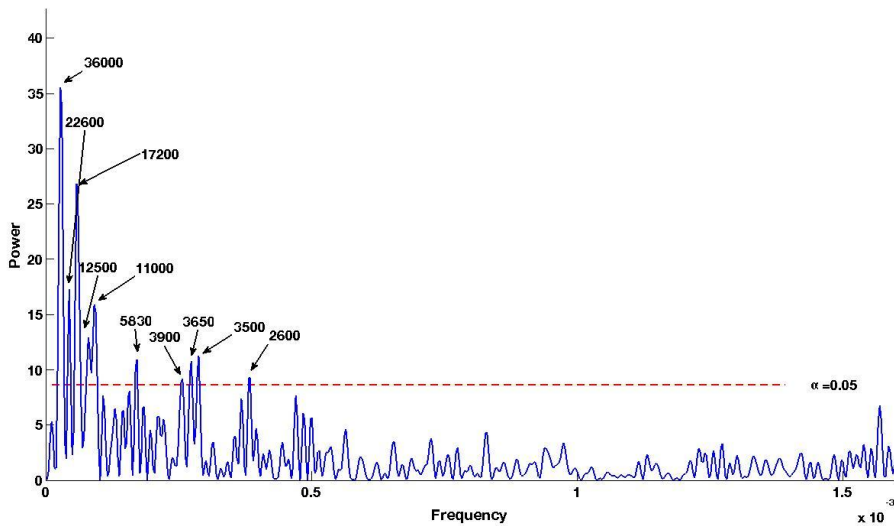


Fig. 3.3. Normalized LSP of the TOC data, filtered by simple moving average over three consecutive samples, spanning the last 90400 years. The average interval of the data is 315 years. The dashed line shows 95% confidence level.

TIC represents the inorganic carbon content in the lake which depends on biogenic and terrestrial carbonate (Li and Ku, 1997; Akçer Ön, 2011). Spectral analysis of TIC data gives periodicities of 30100, 21300, 16450, 11660, 10650 and 3650 years (Fig. 3.4).

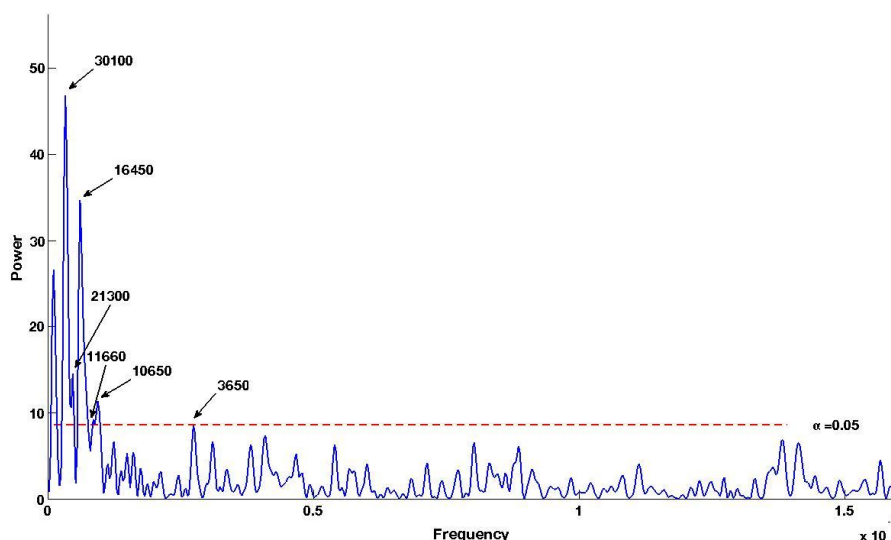


Fig. 3.4. Normalized LSP of the TIC data, filtered by simple moving average over three consecutive samples, spanning the last 90400 years. The average interval of the data is 315 years. The dashed line shows 95% confidence level.

3.1.2. Spectral analysis results of 0-13.5 ka interval

For all the data, spanning the last ~13.5 ka, we preferred the simple moving average of order 50 and resampled every one element of the data from 50 consecutive elements. The statistically significant, over 95% confidence interval, periods are listed below.

It is shown that calcium may be an indicator of past climates (Richter et al., 2006). We use calcium normalized to titanium (Ca/Ti) to normalize with the detrital input and to get a better indicator of biogenic calcium (Akçer Ön, 2011; Çağatay et al., 2013). Spectral analysis of Ca/Ti gives periodicities of 2450, 2000, 1540, 1225, 1020, 885 and 770 years (Fig. 3.5).

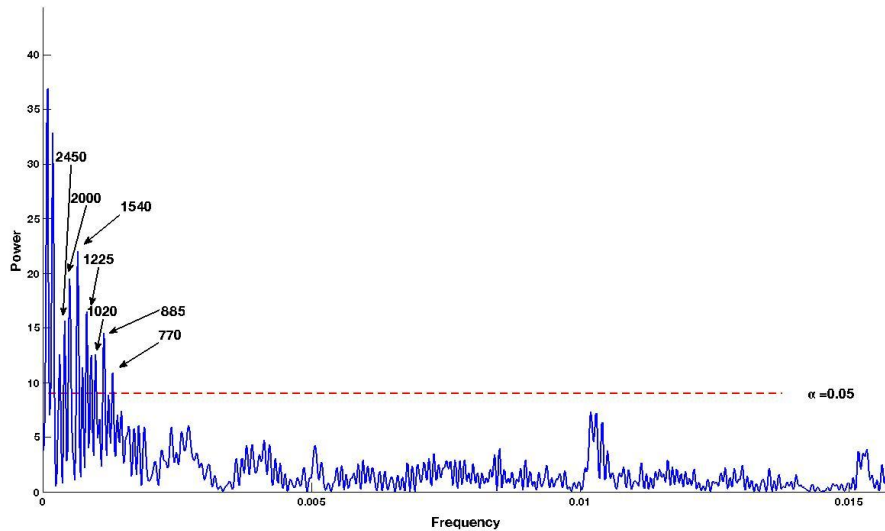


Fig. 3.5. Normalized LSP of the Ca/Ti data, spanning the last 13500 years, filtered by simple moving average over fifty consecutive samples and sampled one sample from every fifty consecutive data, making the average sample interval 19 years. The dashed line shows 95% confidence level.

Strontium normalized to calcium is an indicator of evaporative process since aragonite prefers strontium as a constituent, whereas calcite prefers magnesium (Cohen, 2003). Spectral analysis of Sr/Ca gives periodicities of 2550, 1580, 1150, 830, 690, 550 and 480 years (Fig. 3.6).

Manganese normalized to Titanium (Mn/Ti) is a redox indicator (Çağatay et al., 2013). Spectral analysis of Mn/Ti gives periodicities of 1500 and 300 years over 95% confidence level, 408 and 273 years over 80% confidence level (Fig. 3.7).

Iron (Fe) is a representative of detrital input and a redox indicator (Richter et al., 2006). Spectral analysis of Fe gives periodicities of 2450, 2073, 1540, 1100, 815, 760, 415 and 370 years (Fig. 3.8).

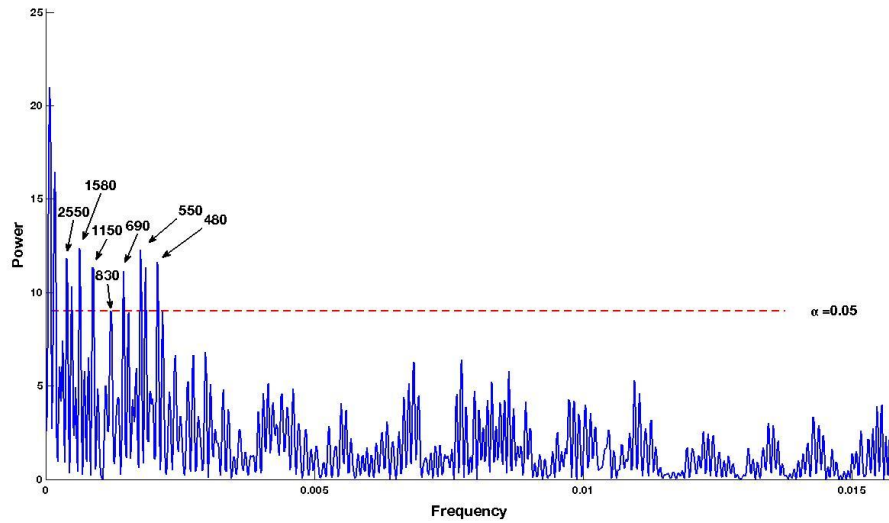


Fig. 3.6. Normalized LSP of the Sr/Ca data, spanning the last 13500 years, filtered by simple moving average over fifty consecutive samples and sampled one sample from every fifty consecutive data, making the average sample interval 19 years. The dashed line shows 95% confidence level.

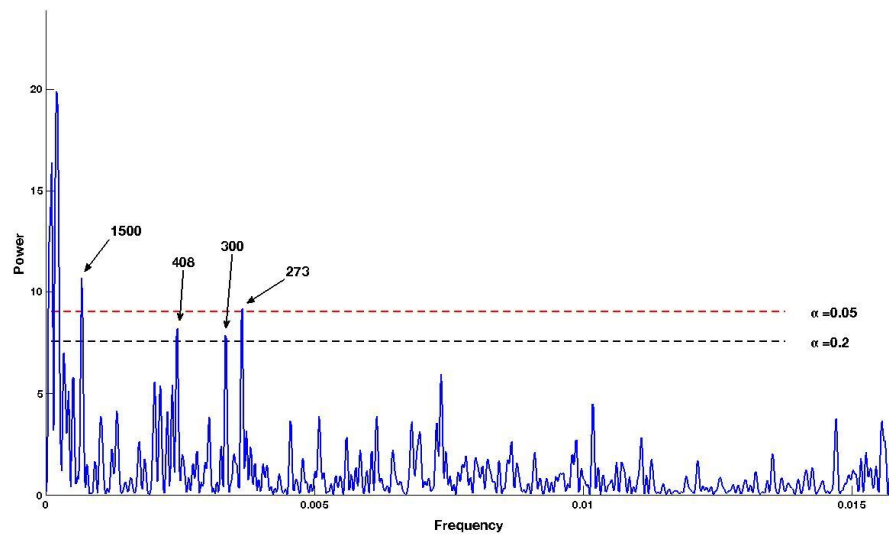


Fig. 3.7. Normalized LSP of the Mn/Ti data, spanning the last 13500 years, filtered by simple moving average over fifty consecutive samples and sampled one sample from every fifty consecutive data, making the average sample interval 19 years. The upper and lower dashed lines show 95% and 80% confidence level respectively.

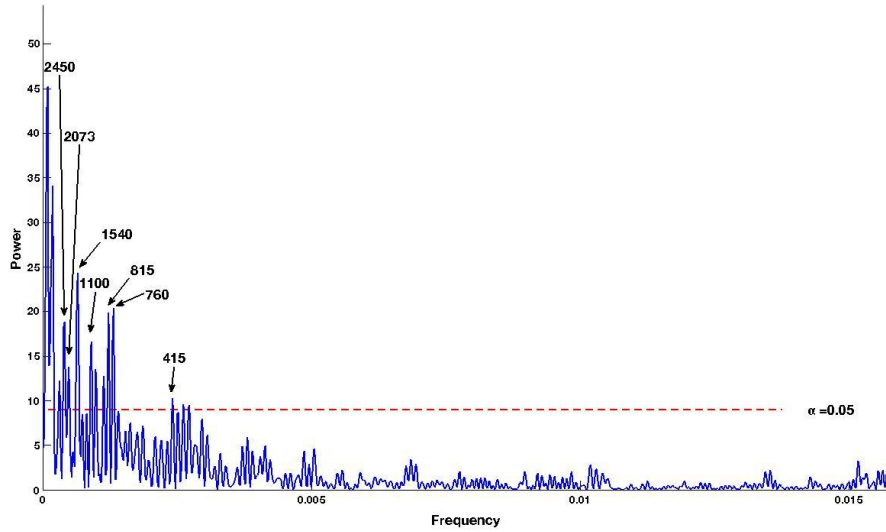


Fig. 3.8. Normalized LSP of the Fe data, spanning the last 13500 years, filtered by simple moving average over fifty consecutive samples and sampled one sample from every fifty consecutive data, making the average sample interval 19 years. The dashed line shows 95% confidence level.

3.1.3. Spectral analysis results of 0-1 ka interval

For all the data, spanning the last ~13.5 ka, we preferred the simple moving average of order 4 and resampled every one element of the data from 4 consecutive elements. The statistically significant, over 95% confidence interval, periods are listed below.

Spectral analysis of Ca/Ti gives periodicities of 195, 126, 83, 64, 41, 33, 22 and 19 years (Fig. 3.9).

Spectral analysis of Sr/Ca gives periodicities of 121, 65, 47, 41, 33, 27 and 19 years (Fig. 3.10).

Spectral analysis of Mn/Ti gives periodicities of 125, 95, 65, 55, 47, 34, 29, 27 and 22 years (Fig. 3.11).

Spectral analysis of Fe gives periodicities of 277, 194, 129, 108, 84, 65, 41, 33 and 27 years (Fig. 3.12).

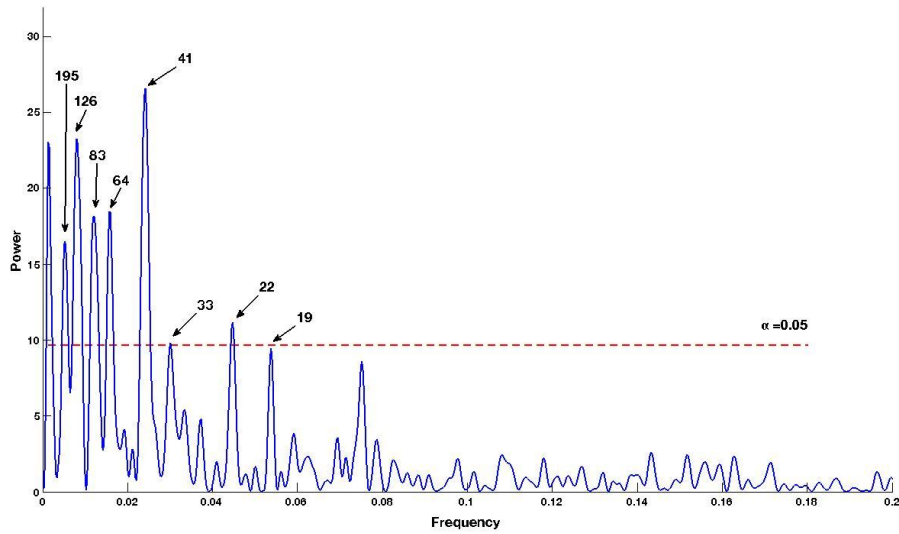


Fig. 3.9. Normalized LSP of the Ca/Ti data, spanning the last 1000 years, filtered by simple moving average over four consecutive samples and sampled one sample from every four consecutive data, making the average sample interval 1.25 years. The dashed line shows 95% confidence level.

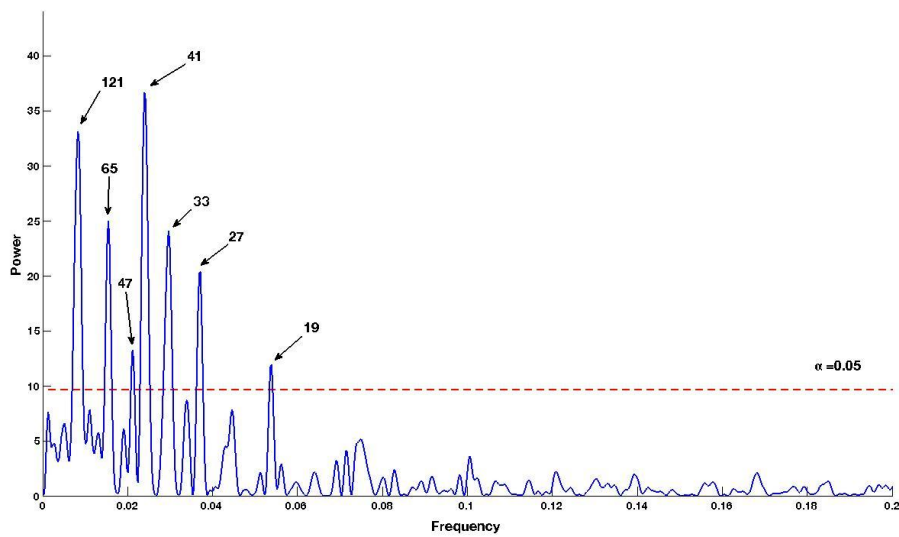


Fig. 3.10. Normalized LSP of the Sr/Ca data, spanning the last 1000 years, filtered by simple moving average over four consecutive samples and sampled one sample from every four consecutive data, making the average sample interval 1.25 years. The dashed line shows 95% confidence level.

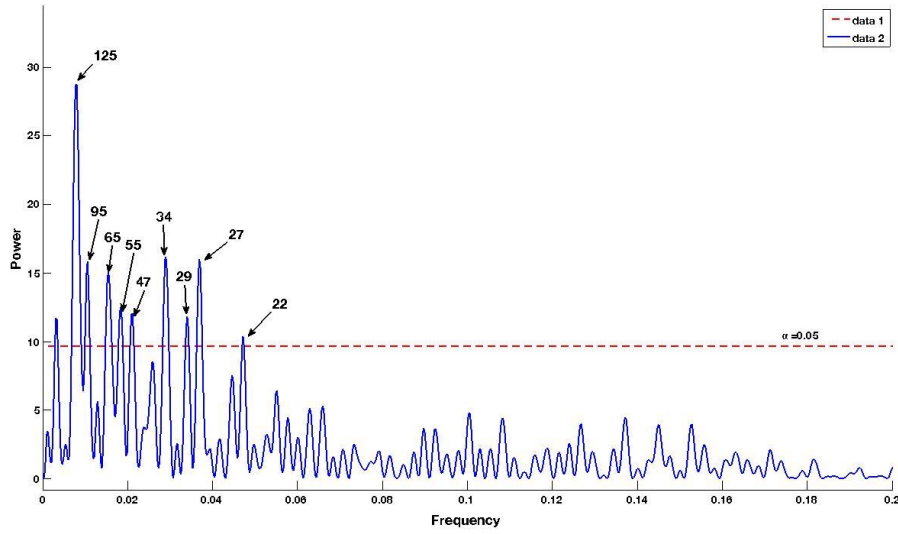


Fig. 3.11. Normalized LSP of the Mn/Ti data, spanning the last 1000 years, filtered by simple moving average over four consecutive samples and sampled one sample from every four consecutive data, making the average sample interval 1.25 years. The dashed line shows 95% confidence level.

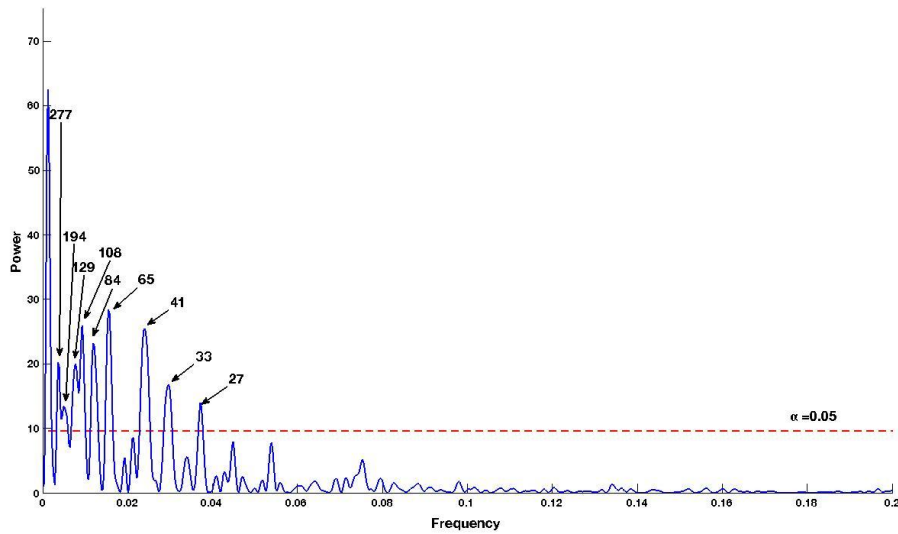


Fig. 3.12. Normalized LSP of the Fe data, spanning the last 1000 years, filtered by simple moving average over four consecutive samples and sampled one sample from every four consecutive data, making the average sample interval 1.25 years. The dashed line shows 95% confidence level.

3.2. Discussion

The periodicities found in this thesis are summarized in Table 3.1.

Table 3.1 Statistically significant spectral peaks (ka) gathered by LSP analysis for the 0-90.4 ka interval in Van5034_1 records. The significance level is chosen to be 95%. “*” denotes the arithmetic mean of two close values mentioned in the results section. B’s on the first column represent the bands.

(0)Van5034_1	$\delta^{18}\text{O}$	$\delta^{13}\text{C}$	TOC	TIC	Mean	Stand. Dev.
B1	33	33	36	30.1	33.025	2.409
B2	21.3	21	22.6	21.3	21.55	0.714
B3		16.5	17.2	16.45	16.717	0.419
B4	12.5	12.5	12.5	11.66	12.29	0.42
B5	10.65	10.3	11	10.65	10.65	0.286
B6	9.05				9.05	-
B7		5.75	5.83		5.79	0.056
B8	4.7	4.15	3.9		4.25	0.409
B9		3.65	3.58*	3.65	3.63	0.04
B10			2.6		2.6	-
B11	1.375				1.375	-

According to their variability I have divided the periodicities into eleven frequency bands and calculated the mean and standard deviation within these bands. The relatively strongest period found in the analyses is ~33 ka. This number may correspond to the change in the obliquity of Milankovitch cycles (~41 ka), because of the relatively short length of ~90 ka record, or it may correspond to 35.4 ka, harmonic of the Milankovitch cycles (Yiou et al., 1994). In my opinion, since it is more powerful than the adjacent precession peak it is the obliquity cycle. The second band with a mean ~21.5 ka is clearly the precession of the equinoxes cycle. In relatively long records, it shows up as two distinct spectral peaks, namely 23 and 19 ka, but in relatively shorter cycles it may show up as a single 21.7 ka peak, as in our situation (Ruddiman, 2008). But there is one question here to be answered, which we couldn't find it. Our results show that the precession cycle is relatively weaker than the right sided neighboring peaks (~16.7 ka) in the analyses except the oxygen isotope data, which should have to show more power according to global results, if it is the obliquity cycle,

Furthermore the other dominant peaks through the analyses are 16.7, 12.3, 10.7, 9, 5.8, 4.3, 3.6, 2.6 and 1.4 ka. It seems, more or less, all of these significant peaks except 1.4 ka lie in the Ghil and Le Treut model GLT (Table 3.2). Also Short et al. (1991) argue that a ~10 ka and a ~12 ka climatic cycle must persist on equatorial regions according to their energy balance climate model, however they add that tropical convective processes may export these oscillations to higher latitudes.

Table 3.2 Theoretical periods of GLT which correlate with our results.

	Corresponding combinations of f_1 (19 ka), f_2 (23 ka) and f_3 (41 ka)	GLT	
B1	f_3	41	
B2	$f_1 \cdot f_3$	35.4	
B3	$f_2 \& f_1$	23	19
B4	$2f_1 \cdot f_2$	16.2	
B5	$2f_1 \cdot f_3$	12.36	
B6	$f_1 + f_2$	10.4	
B7	$2f_2 + f_3$	9	
B8	$4f_2$	5.75	
B9	$4f_1 + f_3$	4.26	
B10	$3f_1 + 3f_2$	3.46	
B11	$2f_1 + 5f_2 + 2f_3$	2.69	

There are many different results supporting our results given in Table 3.1 (see Table 3.3 and for locations see Fig. 3.13). These results are gathered from ice core (Yiou et al., 1991; Mayewski et al., 1997), marine core (Pestiaux et al., 1988; Hagelberg et al., 1994; Yiou et al., 1994; Wara et al., 2000), pollen (Mommersteeg et al., 1995), and Neogene lake sediment data (Kloosterboer-van Hove et al., 2006; Weber et al., 2010).

Table 3.3 Worldwide spectral examples of some previous studies, correlating with our results, numbers are represented in ka. In the uppermost row given numbers represent the references in the following order: (1) Pestiaux et al., 1988, (2) Yiou et al., 1991, (3) Hagelberg et al., 1994, (4) Yiou et al., 1994, (5) Mommersteeg et al., 1995, (6) Mayewski et al., 1997, (7) Ortiz et al., 1999, (8) Wara et al., 2000, (9) Kloosterboer-van Hove et al., 2006, (10) Weber et al., 2010.

	(1)	(2)	(3)	(4)	(5)	(6)	(7)	(8)	(9)	(10)
B1						38				
B2		24 18	23 19	23 19	21 19	22.5				
B3		16		16.1	16					
B4	10.3	14.1	12	12.7	12	11		12.5		
B5		11.1	10	11.3	10.5			10	10	
B6		7.35		9.1			8	8		8
B7		6.57	5	5.9		6.1				
B8	4.7	5.43/4.9		4.9		4.5	5			
B9		3.65				3.2				

Table 3.3. (cont'd)

	(1)	(2)	(3)	(4)	(5)	(6)	(7)	(8)	(9)	(10)
B10	2.5	2.45				2.3			2.5	
B11						1.45			1.5	1.5

Apart from the GLT, the 5.8 ka periodicity may be matched up with a newly found solar variability, which is declared as 6 ka, mentioned by Xapsos and Burke (2009).

2.6 ka periodicity, moreover found by analyses performed on 13.5 ka spanning XRF data as ~2.5 ka, may have different meanings. It exists in GLT model and it may refer to the ~2.3/2.4 ka solar cycle, namely Hallstadtzeit cycle (Damon and Sonnet, 1991; Sonnet et al., 1997; USGS, 2000; Vasiliev and Dergachev, 2002).

The periodicity of ~1.4 ka occurring in oxygen isotope data and in all the XRF data as ~1.55 ka, most probably, correspond to the Dansgaard/Oeschger cycles for Late Pleistocene and Bond cycles for Holocene that are referred in many studies (Bond et al., 1997; Alley, 1998; Bond et al., 1999; Alley et al., 2001; Lockwood, 2001; Schulz, 2002; Hinnov et al., 2002; Rahmstorf, 2003; Wanner and Butikofer, 2008; Turner et al., 2008). The Dansgaard/Oeschger cycles may be an indicator of the region's relation with the North Atlantic. Apart from the 2.5 and 1.5 ka periodicities the ~1.2 ka periodicity also seems to be dominant for the XRF records of the last 13.5 ka (Table 3.4). This periodicity may be a result of North Atlantic thermohaline circulation variability (Chapman and Shackleton, 2000).

Table 3.4 Statistically significant spectral peaks (ka) gathered by LSP analysis for the 0-13.5 ka interval in Van5034_1 records. The significance level is chosen to be 95%. “*” shows the values chosen between 80 and 95% significance level.

	Ca/Ti	Sr/Ca	Mn/Ti	Fe	Mean	Stand. Dev.
B1	2450	2550		2450	2483	58
B2	2000			2073	2037	52
B3	1540	1580	1500	1540	1540	33
B4	1225	1150		1100	1158	63

Table 3.4. (cont'd)

	Ca/Ti	Sr/Ca	Mn/Ti	Fe	Mean	Stand. Dev.
B5	1020				1020	
B6	885	830		815	843	37
B7	770			760	765	7
B8		690			690	
B9		550			550	
B10		480	408*	415	434	40
B11			300*	370	335	49
B12			273		273	

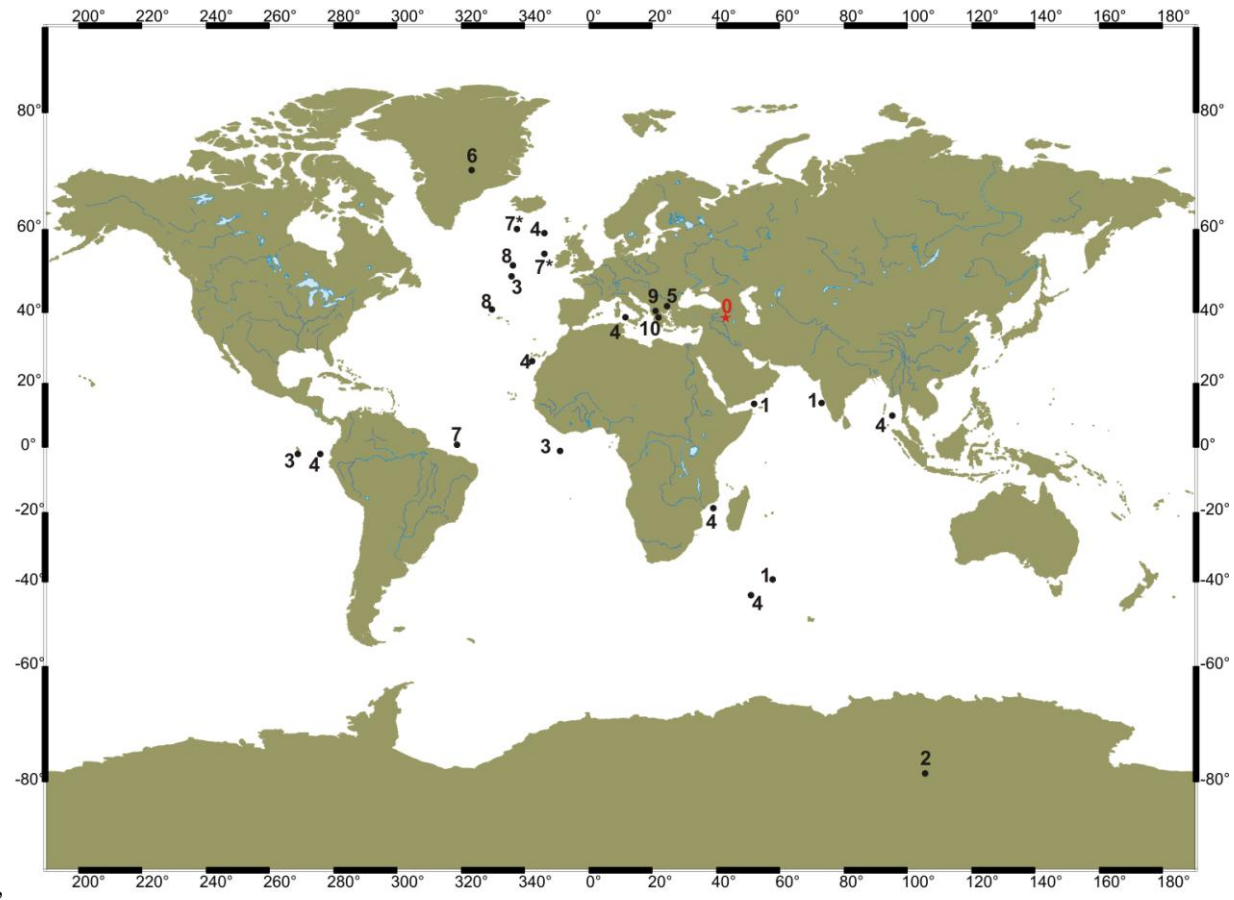


Fig. 3.13 Locations of the previous studies (Table 4.2). The numbers written on the map are a representative of the numbers in front of the names in the Table 4.2. “*” is an indicator of several core samples drilled near the same location.

The results of the spectral analyses performed over the last millennia (Table 3.5) give the 198 year Suess solar cycle, 86 year Gleissberg solar cycle, 22 year Hale solar cycle and 19 year Lunar Saros cycle. Moreover, according to our results, 125, 65, 41 and 33 and 27 year cycles dominate the last 1000 years.

Table 3.5 Statistically significant spectral peaks (ka) gathered by LSP analysis for the 0-1 ka interval in Van5034_1 records. The significance level is chosen to be 95%.

	Ca/Ti	Sr/Ca	Mn/Ti	Fe	Mean	Stand. Dev.
B1				277	277	
B2	195			194	195	0
B3	126	121	125	129	125.3	3.3
B4				108	108	
B5	83		95	84	87.3	6.7
B6	64	65	65	65	64.8	0.5
B7			55		55	
B8		47	47		47	0
B9	41	41		41	41	0
B10	33	33	34	33	33.3	0.5
B11		27	27	27	27	0
B12	22		22		22	0
B13	19	19			19	0

4. CONCLUSIONS

According to this study the results of the spectral analyses of the geochemical data of Lake Van show the following;

1. The ~33 ka periodicity, which is present in the oxygen and carbon isotope, TOC and TIC records, may corresponds to the 41 ka obliquity cycle of Croll-Milankovitch theory or to the 35 ka sub-Milankovitch band of GLT.
2. The ~21.5 ka periodicity present in the records, clearly corresponds to the 21.7 ka precession cycle of Croll-Milankovitch theory.
3. The 16.7, 12.3, 10.65, 9, 5.8, 4.25, 3.6 and 2.6 ka periodicities, have equivalents in GLT as subharmonics of Milankovitch obliquity and precession forcings. Moreover the 5.8 ka periodicity may correspond to 6 ka solar cycle and similarly 2.6 ka periodicity may correspond to 2.4 ka solar cycle, namely Hallstadtzeit cycle.
4. The ~1.5 ka periodicity in oxygen isotope data for the Late Pleistocene stands for the Dansgaard/Oeschger cycles and in XRF data for stands for the Holocene Bond cycles.
5. For the XRF data of the last 13.5 ka years 1200 year periodicity is persistent which may be a result of North Atlantic variability (Olafsdottir, 2010).
6. For the last 1000 years the XRF records show the solar variability cycles which are ~200, 86 and 22 years. Also Lunar Saros cycle (19 years) is being observed in these records.
7. The records of the last 1000 years also show 125, 65, 41 and 33 year periodicities.

Among the periodicities given above cycles of 1200, 125, 65, 41 and 33 years, which are not discussed as global, remain as an enigma. The obvious direction to solve this problem is to use different data around Van region, by this way it would be easier to make comment on these cycles, which may be noise or originated by own dynamics

of the region or related to some other mechanism (see for example; Chapman and Shackleton, 2000; Olafsdottir, 2010).

BIBLIOGRAPHY

Adhémar, J.A. (1842) *Révolution des mers, Déluges périodiques*, Carilian-Goeury et V. Dalmont, Paris, 359p.

Agassiz, L. (1840) *Études sur les glaciers*, Jent & Gassmann, Neuchâtel, 346p.

Akçar, N. and Schluchter, C. (2005) Paleoglaciations in Anatolia: a schematic review and first results, *Eiszeitalter und Gegenwart*, 55(8): 102-121.

Akçer Ön, S. (2011) *Küçükçekmece Lagünü, Yeniçağa, Uludağ Buzul ve Bafa Gölleri'nin (Batı Türkiye) Geç Holosen'deki İklim Kayıtları: Avrupa ve Orta doğu İklim Kayıtları ile Karşılaştırılması*, Ph.D. Thesis, İstanbul Teknik Üniversitesi, İstanbul, 175p.

Allaby, M. (2004) *A Change in the Weather*, Facts On File, NY, 200p.

Alley, R.B. (1998) Icing the North Atlantic, *Nature*, 392(6674): 335-337.

Alley, R.B., Anandakrishnan, S. and Jung, P. (2001) Stochastic resonance in the North Atlantic, *Paleoceanography*, 16(2): 190-198.

Alley, R.B., Anandakrishnan, S. and Jung, P. (2001) Stochastic resonance in the North Atlantic, *Paleoceanography*, 16(2): 190-198.

Andersen, B.G. (1992) Jens Esmark – a pioneer in glacial geology, *Boreas*, 21(1): 97-102.

Andersen, K.K., Azuma, N., Barnola, J.M., Bigler, M., Biscaye, P., Caillon, N., Chappellaz, J., Clausen, H.B., Dahl-Jensen, D., Fischer, H., Fluckiger, J., Fritzsche, D., Fujii, Y., Goto-Azuma, K., Grønvold, K., Gundestrup, N.S., Hansson, M., Huber, C., Hvidberg, C.S., Johnsen, S.J., Jonsell, U., Jouzel, J., Kipfstuhl, S., Landais, A., Leuenberger, M., Lorrain, R., Masson-Delmotte, V., Miller, H., Motoyama, H., Narita, H., Popp, T., Rasmussen, S.O., Raynaud, D., Rothlisberger, R., Ruth, U., Samyn, D., Schwander, J., Shoji, H., Siggard-Andersen, M.L., Steffensen, J.P., Stocker, T., Sveinbjornsdottir, A.E., Svensson, A., Takata, M., Tison, J.L., Thorsteinsson, Th., Watanabe, O., Wilhelms, F. and White, J.W.C. (2004) High-

resolution record of Northern Hemisphere climate extending into the last interglacial period, *Nature*, 431(7005):147-151.

Aydar, E., Gourgaud, A., Ulusoy, I., Digonnet, F., Labazuy, P., Sen, E., Bayhan, H., Kurttas, T. and Tolluoglu, A.U. (2003) Morphological analysis of active Mount Nemrut stratovolcano, eastern Turkey: evidences and possible impact areas of future eruption, *Journal of Volcanology and Geothermal Research*, 123(3-4): 301-312.

Bard, E. (2004) Greenhouse effect and ice ages: historical perspective, *Comptes Rendus Geoscience* 336(7-8): 603-638.

Bard, E., Rostek, F., Turon, J.L. and Gendreau, S. (2000) Hydrological Impact of Heinrich Events in the Subtropical Northeast Atlantic, *Science*, 289(5483): 1321-1324.

Becker, J.S. (2002) State-of-the-art and progress in precise and accurate isotope ratio measurements by ICP-MS and LA-ICP-MS Plenary Lecture, *Journal of Analytical Atomic Spectrometry*, 17(9): 1172-1185.

Becker, J.S. and Dietze, H.J. (2000) Precise and accurate isotope ratio measurements by ICP-MS, *Fresenius J Anal Chem*, 368(1): 23-30.

Berger, A. (1988) Milankovitch Theory and climate, *Reviews of Geophysics*, 26(4): 624-657.

Berger, A. (2012) A Brief History of the Astronomical Theories of Paleoclimates, 107-129, Berger, A., Mesinger, F., Sijacki, D. (editors), *Climate Change*, Springer-Verlag, Wien, 244p.

Bianchi, G.G. and McCave, I.N. (1999) Holocene periodicity in North Atlantic climate and deep-ocean flow south of Iceland, *Nature*, 397(6719): 515-517.

Bloomfield, P. (2000) *Fourier Analysis of Time Series: An Introduction*, 2nd Edition, John Wiley and Sons Inc., NY, 261p.

Bond, G., Broecker, W., Johnsen, S., McManus, J., Labeyrie, L., Jouzel, J. and Bonani, G. (1993) Correlations between climate records from North Atlantic sediments and Greenland ice, *Nature*, 365(6442): 143-147.

Bond, G., Kromer, B., Beer, J., Muscheler, R., Evans, M.N., Showers, W., Hoffmann, S., Lotti-Bond, R., Hajdas, I. and Bonani, G. (2001) Persistent solar influence on North Atlantic climate during the Holocene, *Science*, 294(5549): 2130-2136.

Bond, G., Showers, W., Cheseby, M., Lotti, R., Almasi, P., Priore, P., Cullen, H., Hajdas, I. and Bonani, G. (1997) A pervasive millennial-scale cycle in North Atlantic Holocene and glacial climates, *Science*, 278(5341): 1257-1266.

Bond, G.C., Showers, W., Elliot, M., Evans, M., Lotti, R., Hajdas, I., Bonani, G. and Johnson, S. (1999) The North Atlantic's 1-2 kyr climate rhythm: Relation to Heinrich events, Dansgaard/Oeschger cycles and the Little Ice Age, 35-58, Clark, U., Webb, S. and Keigwin, D. (editors), *Mechanisms of Global Climate Change at Millennial Time Scales*, AGU, Washington DC, 112: 394.

Broecker, W.S., Bond, G., Klas, M., Bonani, G. and Wolfli, W. (1990) A salt oscillator in the glacial Atlantic? 1. The concept, *Paleoceanography*, 5(4): 469-477.

Broecker, W.S. and Denton, G.H. (1989) The role of ocean-atmosphere reorganizations in glacial cycles, *Quaternary Science Reviews*, 9(4): 305-341.

Broecker, W.S. and van Donk, J. (1970) Insolation changes, ice volumes, and the O¹⁸ record in deep-sea cores, *Reviews of Geophysics*, 8(1): 169-198.

Broecker, W.S. (2002) *The Glacial World According to Wally*, 3rd Edition, Eldigio Press, 355p.

Budziak, D., Schneider, R.R., Rostek, F., Müller, P.J., Bard, E. and Wefer, G. (2000) Late Quaternary insolation forcing on total organic carbon and C₃₇ alkenone variations in the Arabian Sea, *Paleoceanography*, 15(3): 307-321.

Çağatay, N., Özeren, M.S., Sarı, E. and Eriş, K.K. (2013) *Van Gölü'nün Geç Pleyistosen-Holosendeki Yüksek Çözünürlüklü Su Seviyesi Salınımları*, TÜBİTAK, Project No.: 108Y279.

Chapman, M.R. and Shackleton, N.J. (2000) Evidence of 550-year and 1000-year cyclicities in North Atlantic circulation patterns during the Holocene, *The Holocene*, 10(3): 287-291.

Chatfield, C. (1996) *The Analysis of Time Series: An Introduction*, 5th Edition, Chapman and Hall/CRC, London, 283p.

Çiftçi, Y., Işık, M.A., Alkeveli, T. and Yeşilova, Ç. (2008) Van Gölü Havzasının Çevre Jeolojisi, *Jeoloji Mühendisliği Dergisi*, 32(2): 45-77.

Clark, P.U., Shakun, J.D., Baker, P.A., Bartlein, P.J., Brewer, S., Brook, E., Carlson, A.E., Cheng, H., Kaufman, D.S., Liu, Z., Marchitto, T.M., Mix, A.C., Morrill, C., Otto-Bliesner, B.L., Pahnke, K., Russell, J.M., Whitlock, C., Adkins, J.F., Blois, J.L., Clark, J., Colman, S.M., Curry, W.B., Flower, B.P., He, F., Johnson, T.C., Lynch-Stieglitz, J., Markgraf, V., McManus, J., Mitrovica, J.X., Moreno, P.I. and Williams, J.W. (2012) Global climate evolution during the last deglaciation, *Proceedings of the National Academy of Sciences*, 109(19): E1134-E1142.

Clement, A.C. and Peterson, L.C. (2008) Mechanisms of abrupt climate change of the last glacial period, *Reviews of Geophysics*, 46(4): RG4002.

CLIMAP Project Members, Ruddiman, W.F., Cline, R.M.L., Hays, J.D., Prell, W.L., Moore, T.C., Kipp, N.G., Molino, B.E., Denton, G.H., Hughes, T.J., Balsam, W.L., Brunner, C.A., Duplessy, J.-C., Fastook, J.L., Imbrie, J., Keigwin, L.D., Kellogg, T.B., McIntyre, A., Matthews, R.K., Mix, A.C., Morley, J.J., Shackleton, N.J., Streeter, S.S. and Thompson, P.R. (1984) The last interglacial ocean, *Quaternary Research*, 21(2): 123-224.

Cohen, A.S. (2003) *Paleolimnology: The History and Evolution of Lake Systems*, Oxford University Press, USA, 500p.

Croll, J. (1864) On the physical cause of the change of climate during geological epochs, *Philos Mag*, 28(187): 121–137.

Croll, J. (1867a) On the eccentricity of the Earth's orbit, and its physical relations to the glacial epoch, *Philos Mag*, 33(221): 119–131.

Croll, J. (1867b) On the change in the obliquity of the ecliptic, its influence on the climate of the polar regions and on the level of the sea, *Philos Mag*, 33: 426–445

.

Croll, J. (1875) *Climate and time in their geological relations: a theory of secular changes of the Earth's climate*, Appleton, New York, 577p.

Cuffey, K.M. and Clow, G.D. (1997) Temperature, accumulation, and ice sheet elevation in central Greenland through the last deglacial transition, *Journal of Geophysical Research: Oceans*, 102(C12): 26383-26396.

Çukur, D., Krastel, S., Demirel-Schluter, F., Demirbağ, E., Imren, C., Niessen, F. and Toker, M. (2013) Sedimentary evolution of Lake Van (Eastern Turkey) reconstructed from high-resolution seismic investigations, *Int J Earth Sci (Geol Rundsch)*, 102(2): 571-585.

Cullen, H.M. and deMenocal, P.B. (2000) North Atlantic influence on Tigris–Euphrates streamflow, *International Journal of Climatology*, 20(8): 853-863.

Damon, P.E. and Sonett, C.P. (1991) Solar and terrestrial components of the atmospheric ^{14}C variation spectrum, 360-388, Sonett, C.P., Giampapa, M.S. and Matthews, M.S. (editors), *The Sun in Time*, The University of Arizona Press, USA, 990p.

Dansgaard, W., Johnsen, S., Clausen, H., Dahl-Jensen, D., Gundestrup, N., Hammer, C. and Oeschger, H. (1984) North Atlantic climatic oscillations revealed by deep Greenland ice cores, 288-298, (editors), *Climate Processes and Climate Sensitivity*, AGU, Washington DC, 29: 368p.

Dansgaard, W., Johnsen, S., Clausen, H., Dahl-Jensen, D., Gundestrup, N., Hammer, C., Hvidberg, C., Steffensen, J., Sveinbjornsdottir, A. and Jouzel, J. (1993) Evidence for general instability of past climate from a 250-kyr ice-core record, *Nature*, 364(6434): 218-220.

Dansgaard, W., Oeschger, H. and Langway, C.C. (1983) Ice Core Indications of Abrupt Climatic Changes, 72-73, Ghazi, A. (editors), *Palaeoclimatic Research and Models*, Springer Netherlands: 205p.

Darwin, C. (1872) *On the origin of species by means of natural selection*, 6th Edition, D. Appleton, New York, 470p.

Davies, G.L. (1968) Another forgotten pioneer of the glacial theory: James Hutton, *J. Glaciol.*, 7(49): (1726-97).

de Charpentier, J. (1836) Account of one of the most important results of the investigations of M. Venetz, regarding the present and earlier condition of the glaciers of the Canton du Valais, *Edinb. New Philos. J.* 21: 210–220.

de Charpentier, J. (1837) Some conjectures regarding the great revolutions which have so changed the surface of Switzerland and particularly that of Canton de Vaud, as to give rise of its present aspect, *Edinb. New Philos. J.* 22: 27–36.

Degens, E.T. and Kurtman, F. (1978) *The geology of lake Van*, Maden Tetkik ve Arama Enstitüsü Yayınları, Ankara, 158p.

Degens, E.T., Wong, H.K., Kempe, S. and Kurtman, F. (1984) A geological study of lake van, Eastern Turkey, *Geol Rundsch*, 73(2): 701-734.

Denton, G.H. (1999) Cenozoic Climate Change, 94-114, Bromage, T.G. and Schrenk F. (editors), *African Biogeography, Climate Change, and Human Evolution*, Oxford University Press, NY, 496p.

Dewey, J.F., Hempton, M.R., Kidd, W.S.F., Şaroglu, F. and Şengör, A.M.C. (1986) Shortening of continental lithosphere: the neotectonics of Eastern Anatolia - a young collision zone, *Geological Society, London, Special Publications*, 19(1): 1-36.

Ehrmann, W.U. and Mackensen, A. (1992) Sedimentological evidence for the formation of an East Antarctic ice sheet in Eocene/Oligocene time, *Palaeogeography, Palaeoclimatology, Palaeoecology*, 93(1-2): 85-112.

Elkatmış, M.N. (2008) Van İlinin Meteorolojik Faktörler Açısından İklim Özellikleri, *Van Gölü Hidrolojisi ve Kirliliği Konferansı*, 21-22 Ağustos, Van, Büyük Ofset ve Matbaacılık, 55-56.

Emiliani, C. (1955) Pleistocene Temperatures, *The Journal of Geology*, 63(6): 538-578.

Erol, O. (2011) *Genel Klimatoloji*, 9. Baskı, Çantay Kitabevi, İstanbul, 445p.

Esmark, J. (1827) Remarks tending to explain the geological history of the Earth, *Edinb. New Philos. J.*, 2: 107–121.

Fleitmann, D., Burns, S.J., Mudelsee, M., Neff, U., Kramers, J., Mangini, A. and Matter, A. (2003) Holocene Forcing of the Indian Monsoon Recorded in a Stalagmite from Southern Oman, *Science*, 300(5626): 1737-1739.

Fleitmann, D., Cheng, H., Badertscher, S., Edwards, R.L., Mudelsee, M., Göktürk, O.M., Fankhauser, A., Pickering, R., Raible, C.C., Matter, A., Kramers, J. and Tüysüz, O. (2009) Timing and climatic impact of Greenland interstadials recorded in stalagmites from northern Turkey, *Geophysical Research Letters*, 36(19).

Forbes, J.D. (1843) *Travels through the Alps of Savoy and other parts of the Pennine chain, with observations on the phenomena of glaciers*, A. and C. Black, Edinburgh, 424p.

Ganopolski, A. and Rahmstorf, S. (2002) Abrupt Glacial Climate Changes due to Stochastic Resonance, *Physical Review Letters*, 88(3): 038501.

Gat, J.R. (2010) *Isotope Hydrology: A Study of the Water Cycle*, Imperial College Press, London, 189p.

Geological Survey (U.S.) (2000) *The Sun and Climate*, USGS Fact Sheet, 095-00, USA, 6p.

Ghil, M. (1994) Cryothermodynamics: the chaotic dynamics of paleoclimate, *Physica D: Nonlinear Phenomena*, 77(1-3): 130-159.

Ghil, M. and Le Treut, H. (1981) A climate model with cryodynamics and geodynamics, *Journal of Geophysical Research: Oceans* 86(C6): 5262-5270.

Ghil, M., Childress, S. (1987) *Topics in Geophysical Fluid Dynamics: Atmospheric Dynamics, Dynamo Theory, and Climate Dynamics*, Springer-Verlag, NY, 485p.

Saragiotis, C. (2008) One dimensional sliding-window arithmetic average of a signal, *MATLAB Central File Exchange*. Retrieved from <http://www.mathworks.com/matlabcentral/fileexchange/1967-slidingavg>

Göktürk, O.M. (2005) *North Sea – Caspian Pattern and its Influence on the Hydrometeorological Parameters over Turkey*, M.Sc. Thesis, İstanbul Teknik Üniversitesi, İstanbul, 44p.

Gradstein, F.M., Ogg, J.G., Schmitz, M.D. and Ogg, G.M. (2012) *The Geologic Time Scale 2012*, Elsevier Publishing, Oxford, 1176p.

Gray, L., Haigh, J. and Harrison, R. (2005) The influence of solar changes on the Earth's climate, *Hadley Centre technical note*, 62: 1-81.

Grubic, A. (2006) The astronomic theory of climatic changes of Milutin Milankovich, *Episodes*, 29 (3): 197-203.

Gündüz, M. and Özsoy, E. (2005) Effects of the North Sea Caspian pattern on surface fluxes of Euro-Asian-Mediterranean seas, *Geophysical Research Letters*, 32(21): L21701.

Hagelberg, T.K., Bond, G. and deMenocal, P. (1994) Milankovitch band forcing of sub-Milankovitch climate variability during the Pleistocene, *Paleoceanography*, 9(4): 545-558.

Harding, A., Palutikof, J. and Holt, T. (2009) The Climate System, 69-88, Woodward, J. (editors), *The Physical Geography of the Mediterranean*, Oxford University Press, Oxford, 663p.

Hays, J.D., Imbrie, J. and Shackleton, N.J. (1976) Variations in the Earth's Orbit: Pacemaker of the Ice Ages, *Science* 194(4270): 1121-1132.

Heinrich, H. (1988) Origin and consequences of cyclic ice rafting in the Northeast Atlantic Ocean during the past 130,000 years, *Quaternary Research*, 29(2): 142-152.

Hemming, S.R. (2004) Heinrich events: Massive late Pleistocene detritus layers of the North Atlantic and their global climate imprint, *Reviews of Geophysics*, 42(1): RG1005.

Hinnov, L.A., Schulz, M. and Yiou, P. (2002) Interhemispheric space-time attributes of the Dansgaard-Oeschger oscillations between 100 and 0 ka, *Quaternary Science Reviews*, 21(10): 1213-1228.

Hoerling, M., Human, K. and Deluisi, B. (Mar. 26, 2010) Forensic Meteorology Solves the Mystery of Record Snows, *Climate Watch Magazine*. Retrieved from <http://www.climatewatch.noaa.gov/article/2010/forensic-meteorology-solves-the-mystery-of-record-snows>.

Horne, J.H. and Baliunas, S.L. (1986) A prescription for period analysis of unevenly sampled time series, *The Astrophysical Journal*, 302: 757-763.

Hoyt, D.V. and Schatten, K.H. (1997) *The Role of the Sun in Climate Change*, Oxford University Press, NY, 279p.

Huguet, C., Fietz, S., Moraleda, N., Litt, T., Heumann, G., Stockhecke, M., Anselmetti, F.S. and Sturm, M. (2012) A seasonal cycle of terrestrial inputs in Lake Van, Turkey, *Environ Sci Pollut Res*, 19(8): 3628-3635.

Hurrell, J.W. (1995) Decadal Trends in the North Atlantic Oscillation: Regional Temperatures and Precipitation, *Science*, 269(5224): 676-679.

Hurrell, J.W., Kushnir, Y. and Visbeck, M. (2001) The North Atlantic Oscillation, *Science*, 291(5504): 603-605.

Hutton, J. (1795) *The theory of the Earth, with proofs and illustrations*, Cadell and Davies.

Imbrie, J. (1982) Astronomical theory of the Pleistocene ice ages: A brief historical review, *Icarus*, 50(2-3): 408-422.

Imbrie, J. and Imbrie, J.Z. (1980) Modeling the Climatic Response to Orbital Variations, *Science*, 207(4434): 943-953.

Imbrie, J., Berger, A., Boyle, E.A., Clemens, S.C., Duffy, A., Howard, W.R., Kukla, G., Kutzbach, J., Martinson, D.G., McIntyre, A., Mix, A.C., Molfino, B., Morley, J.J., Peterson, L.C., Pisias, N.G., Prell, W.L., Raymo, M.E., Shackleton, N.J. and Toggweiler, J.R. (1993) On the structure and origin of major glaciation cycles 2. The 100,000-year cycle, *Paleoceanography*, 8(6): 699-735.

Jones, M.D., Roberts, C.N., Leng, M.J. and Türkeş, M. (2006) A high-resolution late Holocene lake isotope record from Turkey and links to North Atlantic and monsoon climate, *Geology*, 34(5): 361-364.

Jones, P.D., Jonsson, T. and Wheeler, D. (1997) Extension to the North Atlantic oscillation using early instrumental pressure observations from Gibraltar and south-west Iceland, *International Journal of Climatology*, 17(13): 1433-1450.

Kadioğlu, M., Şen, Z. and Batur, E. (1997) The greatest soda-water lake in the world and how it is influenced by climatic change, *Annales Geophysicae*, 15(11): 1489-1497.

Kallen, E., Crafoord, C. and Ghil, M. (1979) Free Oscillations in a Climate Model with Ice-Sheet Dynamics, *Journal of the Atmospheric Sciences*, 36(12): 2292-2303.

Kempe, S., Khoo, F. and Gürleyik, Y. (1978) Hydrography of Lake Van and its drainage area, 30-44, Degens, E.T. and Kurtman, F. (editors), *The Geology of Lake Van*, Maden Tetkik ve Arama Enstitüsü Yayınları, Ankara, 158p.

Keskin, M. (2003) Magma generation by slab steepening and breakoff beneath a subduction-accretion complex: An alternative model for collision-related volcanism in Eastern Anatolia, Turkey, *Geophysical Research Letters*, 30(24): 8046.

Kipfer, R., Aeschbach-Hertig, W., Baur, H., Hofer, M., Imboden, D.M. and Signer, P. (1994) Injection of mantle type helium into Lake Van (Turkey): the clue for quantifying deep water renewal, *Earth and Planetary Science Letters*, 125(1-4): 357-370.

Kloosterboer-van Hoeve, M.L., Steenbrink, J., Visscher, H. and Brinkhuis, H. (2006) Millennial-scale climatic cycles in the Early Pliocene pollen record of Ptolemais, northern Greece, *Palaeogeography, Palaeoclimatology, Palaeoecology*, 229(4): 321-334.

Kurtman, F. and Başkan, E. (1978) Mineral and thermal waters in the vicinity of Lake Van, 50-55, Degens, E.T. and Kurtman, F. (editors), *The Geology of Lake Van*, Maden Tetkik ve Arama Enstitüsü Yayınları, Ankara, 158p.

Kutiel, H. and Benarorch, Y. (2002) North Sea-Caspian Pattern (NCP) - an upper level atmospheric teleconnection affecting the Eastern Mediterranean: Identification and definition, *Theor Appl Climatol*, 71(1-2): 17-28.

Kutiel, H. and Türkeş, M. (2005) New Evidence for The Role of The North Sea — Caspian Pattern on The Temperature and Precipitation Regimes in Continental Central Turkey, *Geografiska Annaler: Series A, Physical Geography*, 87(4): 501-513.

Kutiel, H., Maheras, P., Türkeş, M. and Paz, S. (2002) North Sea - Caspian Pattern (NCP) - an upper level atmospheric teleconnection affecting the eastern Mediterranean - implications on the regional climate, *Theor Appl Climatol*, 72(3-4): 173-192.

Kuzucuoğlu, C., Christol, A., Mouralis, D., Doğu, A.F., Akköprü, E., Fort, M., Brunstein, D., Zorer, H., Fontugne, M., Karabıyıkoglu, M., Scaillet, S., Reyss, J.L.

and Guillou, H. (2010) Formation of the Upper Pleistocene terraces of Lake Van (Turkey), *Journal of Quaternary Science*, 25(7): 1124-1137.

Lamy, F., Arz, H.W., Bond, G.C., Bahr, A. and Pätzold, J. (2006) Multicentennial-scale hydrological changes in the Black Sea and northern Red Sea during the Holocene and the Arctic/North Atlantic Oscillation, *Paleoceanography*, 21(1).

Landmann, G. (1996) *Van See / Türkei: Sedimentologie, Warvenchronologie und Paläoklima der letzten 15 000 Jahre*, PhD Thesis, Universität Hamburg, Hamburg, 123p.

Landmann, G., Reimer, A., Lemcke, G. and Kempe, S. (1996a) Dating Late Glacial abrupt climate changes in the 14,570 yr long continuous varve record of Lake Van, Turkey, *Palaeogeography, Palaeoclimatology, Palaeoecology*, 122(1-4): 107-118.

Landmann, G., Reimer, A. and Kempe, S. (1996b) Climatically induced lake level changes at Lake Van, Turkey, during the Pleistocene/Holocene Transition, *Global Biogeochemical Cycles*, 10(4): 797-808.

Le Treut, H. and Ghil, M. (1983) Orbital forcing, climatic interactions, and glaciation cycles, *Journal of Geophysical Research: Oceans*, 88(C9): 5167-5190.

Le Treut, H., Portes, J., Jouzel, J. and Ghil, M. (1988) Isotopic modeling of climatic oscillations: Implications for a comparative study of marine and ice core records, *Journal of Geophysical Research: Atmospheres* 93(D8): 9365-9383.

Lean, J. (2005) Living with a Variable Sun, *Physics Today*, 58(6): 32-38.

Leng, M., Lamb, A., Heaton, T.E., Marshall, J., Wolfe, B., Jones, M., Holmes, J. and Arrowsmith, C. (2006) Isotopes in Lake Sediments, 147-184, Leng, M. (editors), *Isotopes in Palaeoenvironmental Research*, Springer Netherlands 10: 307p.

Li, H.C. and Ku, T.L. (1997) $\delta^{13}\text{C}$, $\delta^{18}\text{O}$ covariance as a paleohydrological indicator for closed-basin lakes, *Palaeogeography, Palaeoclimatology, Palaeoecology*, 133(1-2): 69-80.

Litt, T., Anselmetti, F.S., Baumgarten, H., Beer, J., Çağatay, N., Cukur, D., Damcı, E., Glombitza, C., Haug, G., Heumann, G., Kallmeyer, J., Kipfer, R., Krastel, S., Kwiecien, O., Meydan, A.F., Örçen, S., Pickarski, N., Randlett, M. E., Schmincke, H.U., Schubert, C.J., Sturm, M., Sumita, M., Stockhecke, M.,

Tomonaga, Y. and PALEOVAN Scientific Team (2012) 500,000 Years of Environmental History in Eastern Anatolia: The PALEOVAN Drilling Project, *Scientific Drilling*, 14: 18-29.

Litt, T., Krastel, S., Örçen, S. and Karabıykoğlu, M. (2007) Lake Van Drilling Project: A Long Continental Record in Eastern Turkey, *Scientific Drilling*, 4: 40-41.

Litt, T., Krastel, S., Sturm, M., Kipfer, R., Örçen, S., Heumann, G., Franz, S.O., Ülgen, U.B. and Niessen, F. (2009), "PALEOVAN", International Continental Scientific Drilling Program (ICDP): site survey results and perspectives, *Quaternary Science Reviews*, 28(15-16): 1555-1567.

Lockwood, J.G. (2001) Abrupt and sudden climatic transitions and fluctuations: a review, *International Journal of Climatology*, 21(9): 1153-1179.

Lockyer, J.N. (1872) The Meteorology of the Future, *Nature*, 7: 98-101.

Lomb, N.R. (1976) Least-squares frequency analysis of unequally spaced data, *Astrophys Space Sci*, 39(2): 447-462.

Lorius, C., Merlivat, L., Jouzel, J. and Pourchet, M. (1979) A 30,000 year isotope climatic record from Antarctic ice, *Nature*, 280: 644-648.

Mayewski, P.A., Meeker, L.D., Twickler, M.S., Whitlow, S., Yang, Q., Lyons, W.B. and Prentice, M. (1997) Major features and forcing of high-latitude northern hemisphere atmospheric circulation using a 110,000-year-long glaciochemical series, *Journal of Geophysical Research: Oceans*, 102(C12): 26345-26366.

Meyers, P.A. (1997) Organic geochemical proxies of paleoceanographic, paleolimnologic, and paleoclimatic processes, *Organic Geochemistry*, 27(5-6): 213-250.

Milankovitch, M. (1941) *Kanon der Erdbastrahlung und seine Anwendung auf des Eiszeitenproblem*. Special Publication 132, Section of Mathematical and Natural Sciences, vol 33, 633p. Belgrade, Royal Serbian Academy of Sciences ('Canon of Insolation and the Ice-Age Problem', translated from German by the Israel Program for Scientific Translations and published for the U.S. Department of Commerce and the National Science Foundation, Washington DC, 1969. Reprinted by Zavod za udzbenike i nastavna sredstva in cooperation with Muzej nauke i tehnike Srpske akademije nauka i umetnosti, Beograd, 1998).

Miller, K.G., Fairbanks, R.G. and Mountain, G.S. (1987) Tertiary oxygen isotope synthesis, sea level history, and continental margin erosion, *Paleoceanography*, 2(1): 1-19.

Mommersteeg, H., Loutre, M.F., Young, R., Wijmstra, T.A. and Hooghiemstra, H. (1995) Orbital forced frequencies in the 975 000 year pollen record from Tenagi Philippon (Greece), *Climate Dynamics*, 11(1): 4-24.

Muller, R.A. and MacDonald, G.J. (1997) Glacial Cycles and Astronomical Forcing, *Science*, 277(5323): 215-218.

Muller, R.A. and MacDonald, G.J. (2000) *Ice ages and astronomical causes: data, spectral analysis, and mechanisms*, Springer; Praxis Pub., London, 318 p.

Mutlu, H., Güleç, N., Hilton, D.R., Aydın, H. and Halldorsson, S.A. (2012) Spatial variations in gas and stable isotope compositions of thermal fluids around Lake Van: Implications for crust-mantle dynamics in eastern Turkey, *Chemical Geology*, 300-301: 165-176.

Öğretmen, N. (2012) *Paleoenvironmental Changes in Lake Van During the Last Glacial-Holocene*, M.Sc. Thesis, İstanbul Teknik Üniversitesi, İstanbul, 63p.

Ólafsdóttir, K. B. (2010) *Time series analysis based on paleoclimatic proxies from lake sediments in Iceland*, M.Sc. Thesis, University of Iceland, Reykjavik, 77p.

Oldroyd, D. R. (1996) *Thinking About the Earth: A History of Ideas in Geology*, Harvard University Press, 410p.

Ortiz, J., Mix, A., Harris, S. and O'Connell, S. (1999) Diffuse spectral reflectance as a proxy for percent carbonate content in North Atlantic sediments, *Paleoceanography*, 14(2): 171-186.

Peel, M. C., Finlayson, B. L., and McMahon, T. A. (2007) Updated world map of the Köppen-Geiger climate classification, *Hydrol. Earth Syst. Sci.*, 11, 1633-1644.

Penck A., Bruckner E. (1909) *Die Alpen in Eiszeitalter*. Tauchnitz, Leipzig, 1042 p.

Pestiaux, P., Mersch, I., Berger, A. and Duplessy, J.C. (1988) Paleoclimatic variability at frequencies ranging from 1 cycle per 10 000 years to 1 cycle per 1000

years: Evidence for nonlinear behaviour of the climate system, *Climatic Change*, 12(1): 9-37.

Petrovic, A. (2012) Canon of Eccentricity: How Milankovic Built a General Mathematical Theory of Insolation, 131-139, Berger, A., Mesinger, F. and Sijacki, D. (editors), *Climate Change*, Springer Vienna: 244p.

Playfair, J. (1802) *Illustrations of the Huttonian theory of the Earth*, Cadell and Davies, 528p.

Prasad, S., Vos, H., Negendank, J.F.W., Waldmann, N., Goldstein, S.L. and Stein, M. (2004) Evidence from Lake Lisan of solar influence on decadal- to centennial-scale climate variability during marine oxygen isotope stage 2, *Geology*, 32(7): 581-584.

Press, W.H. and Rybicki, G.B. (1989) Fast algorithm for spectral analysis of unevenly sampled data, *The Astrophysical Journal*, 338: 277-280.

Press, W.H., Teukolsky, S.A., Vetterling, W.T. and Flannery, B.P. (2007) *Numerical Recipes 3rd Edition: The Art of Scientific Computing*, Cambridge University Press, Cambridge, 1235p.

Rahmstorf, S. (2003) Timing of abrupt climate change: A precise clock, *Geophysical Research Letters*, 30(10): 1510.

Reimer, P. J., Baillie, M. G. L., Bard, E., Bayliss, A., Beck, J. W., Bertrand, C. J. H., Blackwell, P. G., Buck, C. E., Burr, G. S., Kirsten, B. C., Damon, P. E., Edwards, R. L., Fiarbanks, R. G., Friedrich, M., Guilderson, T. P., Hogg, A. G., Hughen, K. A., Kromer, B., McCormac, G., Manning, S., Ramsey, C. B., Reimer, R. W., von der Plicht, J., and Weyhenmeyer, C. E. (2004) INTCAL04 Terrestrial radiocarbon age calibration, 0–26 cal kyr BP, *Radiocarbon*, 46(3): 1029-1058.

Richter, T.O., van der Gaast, S., Koster, B., Vaars, A., Gieles, R., de Stigter, H.C., De Haas, H. and van Weering, T.C.E. (2006) The Avaatech XRF Core Scanner: technical description and applications to NE Atlantic sediments, 39-50, Rothwell, R.G. (editors), *New Techniques in Sediment Core Analysis*, Geological Society, London, Special Publications, 267(1): 266p.

Roberts, N., Jones, M.D., Benkaddour, A., Eastwood, W.J., Filippi, M.L., Frogley, M.R., Lamb, H.F., Leng, M.J., Reed, J.M., Stein, M., Stevens, L., Valero-Garces, B. and Zanchetta, G. (2008) Stable isotope records of Late Quaternary climate and

hydrology from Mediterranean lakes: the ISOMED synthesis, *Quaternary Science Reviews*, 27(25-26): 2426-2441.

Roberts, N. and Wright Jr., H.E. (1993) Vegetational, Lake-Level, and Climatic History of the Near East and Southwest Asia, 194-220, Wright Jr., H.E., Kutzbach, J.E., Webb III, T., Ruddiman, W.F., Street-Perrott, F.A. and Bartlein, P.J. (editors), *Global Climates since the Last Glacial Maximum*, University of Minnesota Press, Minneapolis, 569p.

Robin, G.D.Q. (1977) Ice Cores and Climatic Change, *Philosophical Transactions of the Royal Society of London. B, Biological Sciences*, 280(972): 143-168.

Rogers, J.C. (1997) North Atlantic Storm Track Variability and Its Association to the North Atlantic Oscillation and Climate Variability of Northern Europe, *Journal of Climate*, 10(7): 1635-1647.

Rohling, E., Mayewski, P., Abu-Zied, R., Casford, J. and Hayes, A. (2002) Holocene atmosphere-ocean interactions: records from Greenland and the Aegean Sea, *Climate Dynamics*, 18(7): 587-593.

Ruddiman, W.F. (2008) *Earth's Climate: Past and Future*, W.H. Freeman and Company, NY, 388p.

Saragiotis, C. (2008) Lomb normalized periodogram, *MATLAB Central File Exchange*. Retrieved from <http://www.mathworks.com/matlabcentral/fileexchange/22215-lomb-normalized-periodogram>

Şaroğlu, F. and Güner, Y. (1981) Doğu Anadolu'nun Jeomorfolojik gelişimine etki eden öğeler; Jeomorfoloji, tektonik, volkonizma ilişkileri, *Türkiye Jeoloji Kurumu Bülteni* 24: 39 – 50.

Savin, S.M., Douglas, R.G. and Stehli, F.G. (1975) Tertiary marine paleotemperatures, *Geological Society of America Bulletin*, 86(11): 1499-1510.

Scargle, J.D. (1982) Studies in astronomical time series analysis. II-Statistical aspects of spectral analysis of unevenly spaced data, *The Astrophysical Journal*, 263: 835-853.

Schulz, M. (2002) On the 1470-year pacing of Dansgaard-Oeschger warm events, *Paleoceanography*, 17(2): 4-1-4-9.

Şengör, A.M.C., Özeren, M.S., Keskin, M., Sakınç, M., Özbakır, A.D. and Kayan, İ. (2008) Eastern Turkish high plateau as a small Turkic-type orogen: Implications for post-collisional crust-forming processes in Turkic-type orogens, *Earth-Science Reviews*, 90(1-2): 1-48.

Şengör, A.M.C., Özeren, S., Genç, T. and Zor, E. (2003) East Anatolian high plateau as a mantle-supported, north-south shortened domal structure, *Geophysical Research Letters*, 30(24): 8045.

Seylaz, L. (1962) A forgotten pioneer of the glacial theory: John Playfair (1748-1819), *J. Glaciol.*, 4(31): 124-126.

Short, D.A., Mengel, J.G., Crowley, T.J., Hyde, W.T. and North, G.R. (1991) Filtering of milankovitch cycles by Earth's geography, *Quaternary Research*, 35(2): 157-173.

Sonett, C.P., Webb, G.M. and Zakharian, A. (1997) The quest for evidence of long-period solar wind variability, 67-110, Jokipii, J.R., Sonett, C.P. and Giampapa, M.S. (editors), *Cosmic Winds and the Heliosphere*, The University of Arizona Press, USA, 1013p.

Stockhecke, M., Anselmetti, F.S., Meydan, A.I.F., Odermatt, D. and Sturm, M. (2012) The annual particle cycle in Lake Van (Turkey), *Palaeogeography, Palaeoclimatology, Palaeoecology*, 333-334: 148-159.

Sumita, M. and Schmincke, H.U. (2013) Impact of volcanism on the evolution of Lake Van II: Temporal evolution of explosive volcanism of Nemrut Volcano (eastern Anatolia) during the past ca. 0.4 Ma, *Journal of Volcanology and Geothermal Research*, 253: 15-34.

Summerfield, M. A. (1991) *Global Geomorphology: An introduction to the study of landforms*, Longman, NY, 537p.

Talbot, M.R. (1990) A review of the palaeohydrological interpretation of carbon and oxygen isotopic ratios in primary lacustrine carbonates, *Chemical Geology: Isotope Geoscience section*, 80(4): 261-279.

Trauth, M. (2010) *MATLAB Recipes for Earth Sciences*, 3rd Edition, Springer-Verlag, Berlin, 336p.

Türkeş, M. (2010) *Klimatoloji ve Meteoroloji*, Kriter Yayınları, İstanbul, 672p.

Turner, R., Roberts, N. and Jones, M.D. (2008) Climatic pacing of Mediterranean fire histories from lake sedimentary microcharcoal, *Global and Planetary Change*, 63(4): 317-324.

Turney, C. (2008) *Ice, Mud and Blood: Lessons from climates past*, Macmillan, NY, 256p.

Turkish State Meteorological Service (2013) *Cities and Holiday Resorts Forecast*. Retrieved from <http://www.dmi.gov.tr/en-US/forecast-cities.aspx?m=VAN> on 03.05.2013.

Ünal, Y., Kindap, T. and Karaca, M. (2003) Redefining the climate zones of Turkey using cluster analysis, *International Journal of Climatology*, 23(9): 1045-1055.

Urey, H.C. (1947) The thermodynamic properties of isotopic substances, *Journal of the Chemical Society (Resumed)*, 562-581.

Vasiliev, S. S. and Dergachev, V. A. (2002) The ~ 2400-year cycle in atmospheric radiocarbon concentration: bispectrum of ¹⁴C data over the last 8000 years, *Ann. Geophys.*, 20: 115-120.

Venez, I. (1821) Mémoire sur les variations de la température des Alpes de la Suisse, *Mém. Soc. Helv. Sci. Nat.*, 1(2): 1-38.

Visbeck, M. (2002) The Ocean's Role in Atlantic Climate Variability, *Science*, 297(5590): 2223-2224.

Visbeck, M.H., Hurrell, J.W., Polvani, L. and Cullen, H.M. (2001) The North Atlantic Oscillation: Past, present, and future, *Proceedings of the National Academy of Sciences*, 98(23): 12876-12877.

Wallace, J.M. and Hobbs, P.V. (2006) *Atmospheric Science*, Academic Press, Amsterdam, 483p.

Wanner, H. and Butikofer, J. (2008) Holocene Bond cycles: real or imaginary?, *Geografie*, 4: 113.

Wara, M.W., Ravelo, A.C. and Revenaugh, J.S. (2000) The pacemaker always rings twice, *Paleoceanography*, 15(6): 616-624.

Weber, M.E., Tougiannidis, N., Kleineder, M., Bertram, N., Ricken, W., Rolf, C., Reinsch, T. and Antoniadis, P. (2010) Lacustrine sediments document millennial-scale climate variability in northern Greece prior to the onset of the northern hemisphere glaciation, *Palaeogeography, Palaeoclimatology, Palaeoecology*, 291(3-4): 360-370.

Wick, L., Lemcke, G. and Sturm, M. (2003) Evidence of Lateglacial and Holocene climatic change and human impact in eastern Anatolia: high-resolution pollen, charcoal, isotopic and geochemical records from the laminated sediments of Lake Van, Turkey, *The Holocene*, 13(5): 665-675.

Wigley, T.M.L. and Farmer, G. (1982) Climate of the Eastern Mediterranean and Near East, 3-37, Bintliff, J.L. and van Zeist, W. (editors), *Palaeoclimates, Palaeoenvironments and Human Communities in the Eastern Mediterranean Region in Later Prehistory*. B.A.R. International Series, vol. 133, 540p.

Wong, H.K. and Degens, E.T. (1979) The bathymetry of Lake Van, eastern Turkey, 6-10, Degens, E.T. and Kurtman, F. (editors), *The Geology of Lake Van*, Maden Tetkik ve Arama Enstitüsü Yayınları, Ankara, 158p.

Wong, H.K. and Finckh, P. (1978) Shallow structures in Lake Van, 20-28, Degens, E.T. and Kurtman, F. (editors), *The Geology of Lake Van*, Maden Tetkik ve Arama Enstitüsü Yayınları, Ankara, 158p.

Xapsos, M.A. and Burke, E.A. (2009) Evidence of 6000-Year Periodicity in Reconstructed Sunspot Numbers, *Sol Phys*, 257(2): 363-369.

Yiou, P., Genthon, C., Ghil, M., Jouzel, J., Le Treut, H., Barnola, J.M., Lorius, C. and Korotkevitch, Y.N. (1991) High-frequency paleovariability in climate and CO₂ levels from Vostok Ice Core Records, *Journal of Geophysical Research: Solid Earth*, 96(B12): 20365-20378.

Yiou, P., Ghil, M., Jouzel, J., Paillard, D. and Vautard, R. (1994) Nonlinear variability of the climatic system from singular and power spectra of Late Quaternary records, *Climate Dynamics*, 9(8): 371-389.

Yılmaz, Y., Güner, Y. and Şaroğlu, F. (1998) Geology of the quaternary volcanic centres of the east Anatolia, *Journal of Volcanology and Geothermal Research*, 85(1-4): 173-210.

Zachos, J., Pagani, M., Sloan, L., Thomas, E. and Billups, K. (2001) Trends, Rhythms, and Aberrations in Global Climate 65 Ma to Present, *Science*, 292(5517): 686-693.

APPENDICES

Appendix A. Ghil and Le Treut model (GLT)

After the successful explanations of climatic oscillations due to external forces on the order of 10^4 and 10^5 years (Milankovitch, 1941; Broecker and van Donk, 1970; Hays et al., 1976) still two problems appearing in the spectral solutions remained to be solved. First is the 100 ka dilemma. This is the 100 ka periodicity of the sediment records, which is theoretically caused by the changes in the eccentricity of the Earth's orbit and theoretically should be the weakest of the three of the astronomical causes, namely precession, obliquity and eccentricity variation, in Milankovitch theory, however eccentricity is observed as a dominant peak rather than the others (Hays et al., 1976; Imbrie and Imbrie, 1980; Imbrie et al., 1993, Muller and MacDonald, 1997; Muller and MacDonald, 2000). The second problem is the periodicities observed in the spectral analysis between the 5 ka and 15 ka band (see Table 4.2). The astronomical theories do not have an explanation for these observed spectral peaks.

Le Treut and Ghil (1983) offer a simplified model to explain these problems. Their model depends on the interactive mechanisms of the atmosphere, ocean, precipitation, ice caps and the visco-elastic behavior of the crust and the upper mantle to ice load variations, which result in a self-sustained oscillating climate system (Kallen et al., 1979; Ghil and Le Treut, 1981; Le Treut and Ghil, 1983; Le Treut et al., 1988; Ghil 1994). GLT is described by three nonlinear equations that describe: (1) the evolution of the globally averaged temperature, (2) the evolution of polar ice caps, (3) the isostatic reply of the crust and the upper mantle to the ice load. The rough explanation of the model's self-sustained oscillating mechanism given by Ghil (1994) is as follows (The symbol " \cong " below should be read as "positively correlated with", not a linear proportionality).

According to energy balance models, overall averaged temperature (T) change of the Earth is negatively correlated with the albedo of the planet (α),

$$\frac{dT}{dt} \cong -\alpha. \quad (\text{A.1})$$

The albedo is defined as the reflectivity of the light and since the effects of the clouds on albedo is not well understood, this model uses the term albedo as surface albedo. It is clear that the change in sea and continental ice is the most responsible of surface albedo, here the albedo used in this model is albedo of the ice (Ghil and Childress, 1987). So albedo increases with the ice volume (V),

$$\alpha \cong V. \quad (\text{A.2})$$

Equations (A.1) and (A.2) gives

$$\frac{dT}{dt} \cong -V. \quad (\text{A.3})$$

The volume of the ice sheets is determined by the net snow and ice precipitation (p) over the ice sheet, that is;

$$\frac{dV}{dt} \cong p, \quad (\text{A.4})$$

and

$$p \cong p_{ac} - p_{ab}, \quad (\text{A.5})$$

where p_{ac} is the net accumulation and p_{ab} is the net ablation. Because of the activation and intensification of the hydrologic cycle, net accumulation rate on ice sheets is positively correlated with the temperature (Robin, 1977, Lorius et al., 1979), i.e.

$$p_{ac} \cong T. \quad (\text{A.6})$$

By assuming that the effect of T on p_{ac} is stronger than the effect of T on p_{ab} , we can rewrite (A.6) as;

$$p \cong T. \quad (\text{A.7})$$

Equations (A.4) and (A.7) gives the following,

$$\frac{dV}{dt} \cong T. \quad (\text{A.8})$$

If we rewrite (A.3) and (A.8) together, it is seen that they form an oscillatory system,

$$\frac{dT}{dt} \cong -V. \quad (\text{A.9})$$

$$\frac{dV}{dt} \cong T. \quad (\text{A.10})$$

Furthermore the isostatic sinking of the bedrock caused by the ice-mass growth move the snow line poleward and reduces the accumulation area. Hence ablation increases with the visco-elastic behavior of the lithosphere. Therefore;

$$\frac{dp}{dt} \cong -V, \quad (\text{A.11})$$

and by rewriting (A.4)

$$\frac{dV}{dt} \cong p, \quad (\text{A.12})$$

we can have another oscillatory system (Ghil and Childress, 1987; Ghil, 1994).

Le Treut and Ghil (1983) simulated an isotope model with the oscillator described in GLT. Taking the orbital frequencies, namely obliquity and precession, as $f_1=1/19 \text{ ka}^{-1}$, $f_2=1/23 \text{ ka}^{-1}$ and $f_3=1/41 \text{ ka}^{-1}$ and used them to calculate the frequencies that the oscillator will create. The spectral power shows that the oscillator creates harmonics and subharmonics of the orbital frequencies, i.e.

$$\sum_{j=1}^3 r_j f_j, \quad (\text{A.13})$$

where r_j is an integer. Moreover with this model they offer an answer to the 100 ka dilemma, that is $f_1-f_2= 1/109 \text{ ka}^{-1}$ (Le Treut and Ghil, 1983; Le Treut et al., 1988, Yiou et al, 1994).

Appendix B. Plots of the 90400 year data

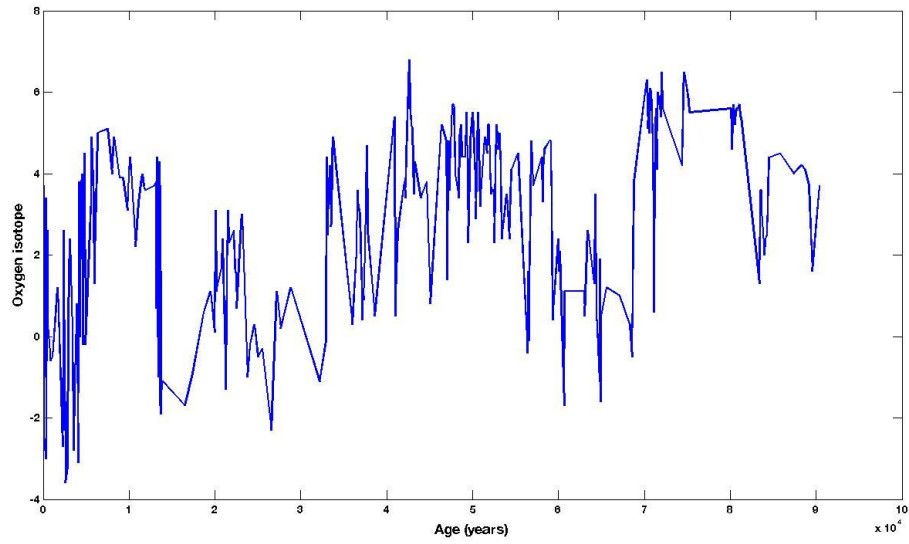


Fig. B1: Plot of $\delta^{18}\text{O}$ data for the last 90400 years.

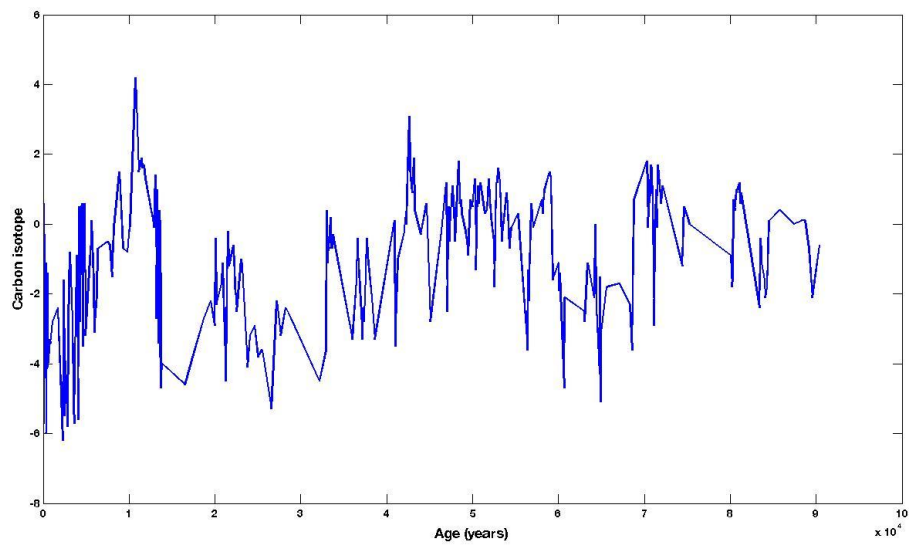


Fig. B2: Plot of $\delta^{13}\text{C}$ data for the last 90400 years.

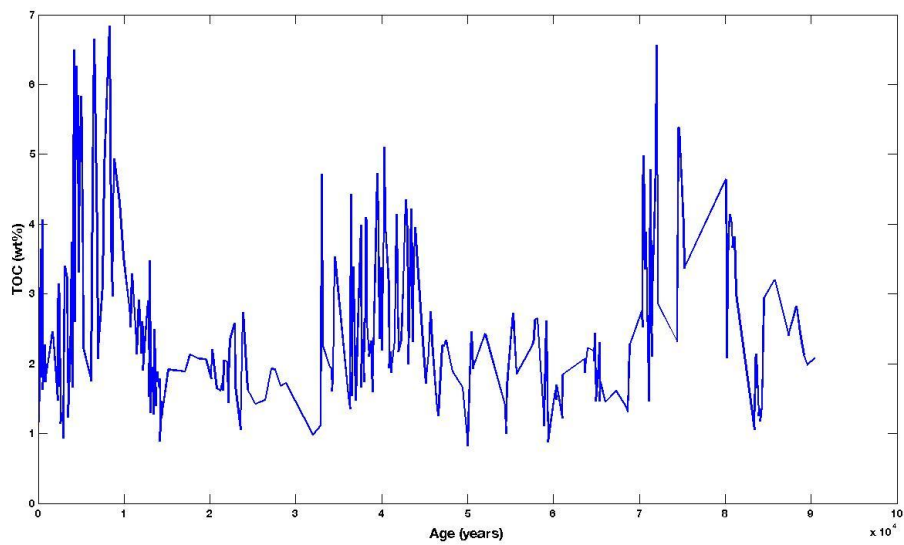


Fig. B3: Plot of TOC data for the last 90400 years.

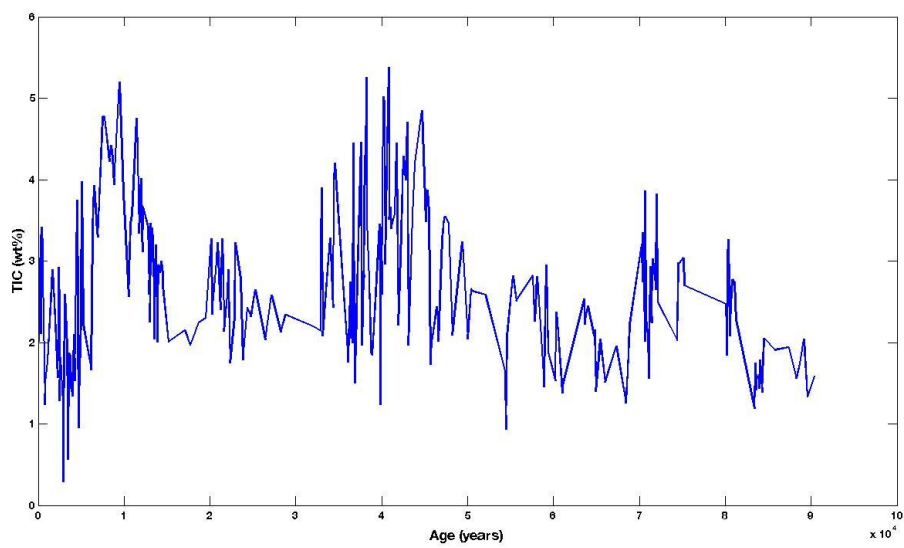


Fig. B4: Plot of TIC data for the last 90400 years.

Appendix C. Plots of the 13500 year XRF data

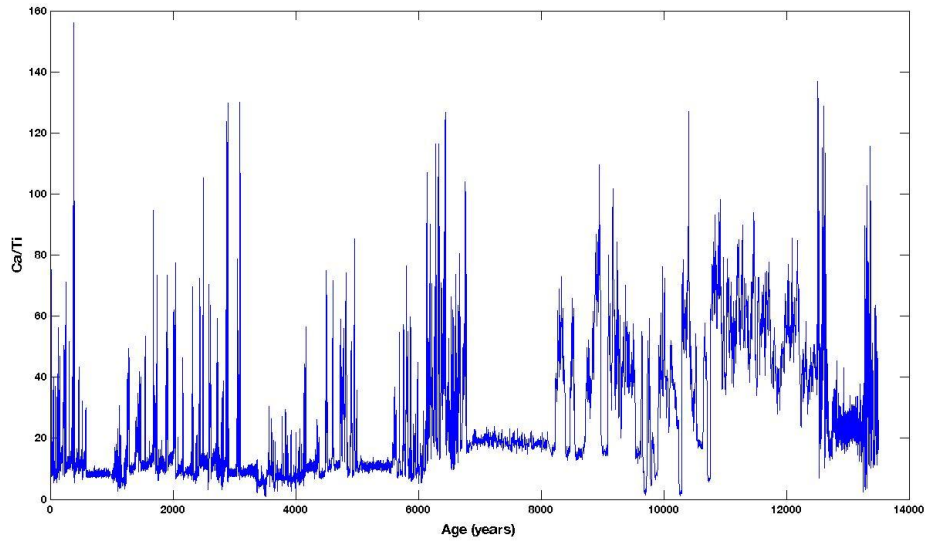


Fig. C1: Plot of Ca/Ti data for the last 13500 years.

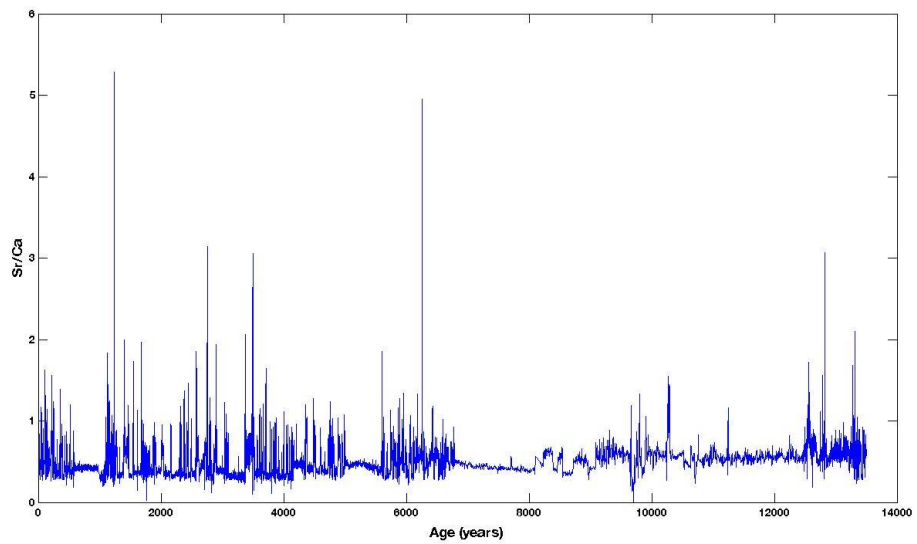


Fig. C2: Plot of Sr/Ca data for the last 13500 years.

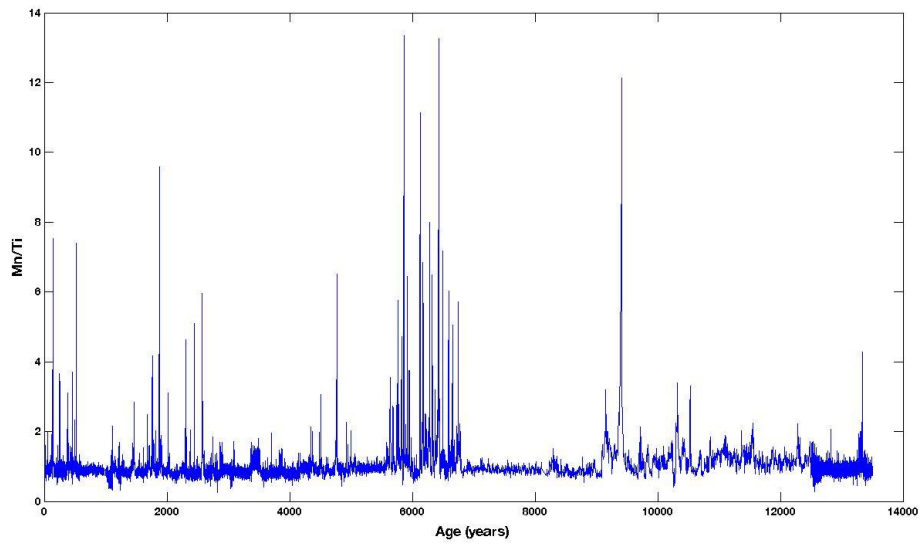


Fig. C3: Plot of Mn/Ti data for the last 13500 years.

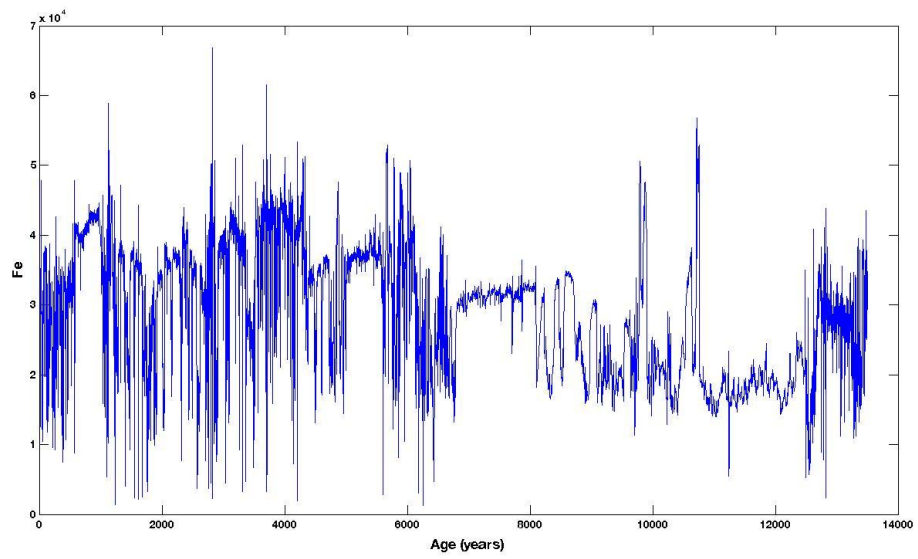


Fig. C4: Plot of Fe data for the last 13500 years.

Appendix D. MATLAB Codes Used in the Thesis

Sliding Average

Below MATLAB algorithm is retrieved from Giugliano (2002).

```
function out = slidingavg(in, N)

if (isempty(in)) | (N<=0)
disp(sprintf('SlidingAvg: (Error) empty input data or N null.));
return;
end
if (N==1)
out = in;
return;
end
nx = length(in);
if (N>=(2*(nx-1)))
out = mean(in)*ones(size(in));
return;
end
out = zeros(size(in));
if rem(N,2)~=1
m = N/2;
else
m = (N-1)/2;
end
for i=1:nx,
if ((i-m) < 1) & ((i+m) <= nx)
out(i) = mean(in(1:i+m));
elseif ((i-m) >= 1) & ((i+m) <= nx)
out(i) = mean(in(i-m:i+m));
elseif ((i-m) >= 1) & ((i+m) > nx)
out(i) = mean(in(i-m:nx));
elseif ((i-m) < 1) & ((i+m) > nx)
out(i) = mean(in(1:nx));
end
end
```

Resampling

```
function [xsampled,tsampled]=sample(x,t,k)

xsampled=zeros(floor(length(x)/k),1);
tsampled=zeros(floor(length(x)/k),1);
for i= 1: (floor(length(x)/k))
xsampled(i)=x(i*k);
```

```

tsampled(i)=t(i*k);
end

```

Fast Algorithm of LSP

Below MATLAB algorithm is retrieved from Saragiotis (2008), which is a translation of the C++ code in Press et al. (2007).

```

function [P,f,alpha] = fastlomb(x,t,varargin)

if nargin < 2,
error('%s: there must be at least 2 inputs.',mfilename);
end
MACC = 10;
[x,t,hifac,ofac,a_usr,f,fig] = init(x,t,varargin{:});
nt = length(t);
mx = mean(x);
x = x-mx;
vx = var(x);
if vx==0,
error('x has zero variance');
end
nf = length(f);
nfreq = 2^nextpow2(ofac*hifac*nt*MACC);
tmin = t(1);
tmax = t(end);
T = tmax-tmin;
fac = 2*nfreq/(T*ofac);
[wk1,wk2] = extirpolate(t-tmin,x,fac,nfreq,MACC);
W = fft(wk1);
reft1 = real(W(2:nf+1));
imft1 = imag(W(2:nf+1));
W = fft(wk2);
reft2 = real(W(2:nf+1));
imft2 = imag(W(2:nf+1));
hypo = sqrt(reft2.^2+imft2.^2);
hc2wt = 0.5*reft2./hypo;
hs2wt = 0.5*imft2./hypo;
cwt = sqrt(0.5+hc2wt);
swt = (sign(hs2wt)+(hs2wt==0)).*(sqrt(0.5-hc2wt));
den = 0.5*nt + hc2wt.*reft2 + hs2wt.*imft2;
cterm = (cwt.*reft1 + swt.*imft1).^2./den;
stern = (cwt.*imft1 - swt.*reft1).^2./(nt-den);
P = (cterm+stern)/(2*vx);
P = P(:);
M = 2*nf/ofac;
alpha = 1 - (1-exp(-P)).^M;
alpha(alpha<0.1) = M*exp(-P(alpha<0.1));

```

```

if fig
figure
styles = {'-', '-.', '--'};
a = [0.05];
La = length(a);
z = -log(1-(1-a).^(1/M));
hold on;
for i=1:La
line([f(1),0.87*f(end)],[z(i),z(i)],'Color','r','LineStyle',styles{ceil(i*3/La)});
text(0.9*f(end),z(i),strcat('\alpha = ',num2str(a(i))),'fontsize',10);
end
if ~isempty(a_usr)
[tmp,ind] = intersect(a_usr,a);
a_usr(ind)=[];
La_usr = length(a_usr);
z_usr = -log(1-(1-a_usr).^(1/M));
for i = 1:La_usr
line([f(1),0.87*f(end)],[z_usr(i),z_usr(i)],'Color','k','LineStyle',styles{ceil(i*3/La_usr)});
text(0.9*f(end),z_usr(i),strcat('\alpha = ',num2str(a_usr(i))),'fontsize',10);
end
end
z = [z z_usr];
end
plot(f,P,'b');
set(gca,'FontSize',12)
title('\bfLSP','fontsize',15)
xlabel('Frequency'); ylabel('Power')
xlim([0 f(end)]); ylim([0,1.2*max([z; P])]);
hold off;
end
end

```

```

function [x,t,hifac,ofac,a,f,fig] = init(x,t,varargin)
if nargin < 6, a = [];
else a = sort(varargin{4});
a = a(:)';
end
if nargin < 5, ofac = 4;
else ofac = varargin{3};
end
if nargin < 4, hifac = 1;
else hifac = varargin{2};
end
if nargin < 3, fig = 0;
else fig = varargin{1};
end
if isempty(ofac),
ofac = 4;

```



```

end
if isempty(hifac),
hifac = 1;
end
if isempty(fig),
fig = 0;
end
if ~isvector(x) || ~isvector(t),
error('%s: inputs x and t must be vectors',mfilename);
else
x = x(:); t = t(:);
nt = length(t);
if length(x)~=nt
error('%s: Inputs x and t must have the same length',mfilename);
end
end
[t,ind] = unique(t);
x = x(ind);
if length(x)~=nt, disp(sprintf('WARNING %s: Double entries have been
eliminated',mfilename));
end
T = t(end) - t(1);
nf = round(0.5*ofac*hifac*nt);
f = (1:nf)/(T*ofac);
end

```

```

function [wk1,wk2] = extirpolate(t,x,fac,nfreq,MACC)
nt = length(x);
wk1 = zeros(2*nfreq,1);
wk2 = zeros(2*nfreq,1);
for j = 1:nt
ck = 1 + mod(t(j)*fac,2*nfreq);
ckk = 1 + mod(2*(ck-1), 2*nfreq);
wk1 = spread(x(j),wk1,ck, MACC);
wk2 = spread(1 ,wk2,ckk,MACC);
end
end

```

```

function yy = spread(y,yy,x,m)

```

```

nfac = [1 1 2 6 24 120 720 5040 40320 362880];
n = length(yy);
if x == round(x)
yy(x) = yy(x) + y;
else
i1 = min([ max([ floor(x-0.5*m+1),1 ]), n-m+1 ]);
i2 = i1+m-1;

```

```
nden = nfac(m);
fac = x-i1;
fac = fac*prod(x - (i1+1:i2));
yy(i2) = yy(i2) + y*fac/(nden*(x-i2));
for j = i2-1:-1:i1
nden = (nden/(j+1-i1))*(j-i2);
yy(j) = yy(j) + y*fac/(nden*(x-j));
end
end
end
```

CURRICULUM VITAE

Zeki Bora Ön was born in İstanbul. He had his high school education in Kadıköy Anadolu High School and then he attended to mathematics in Boğaziçi University. He started his master education at İTÜ and finished it in Muğla Sıtkı Koçman University, Geological Engineering Department in 2013.

Conference Proceedings

Ön, Z.B., Özeren, M.S., Çağatay, M.N., Akçer, S., Damcı, E. and Sancar, Ü. (2013) Van Gölü Çökellerinde Geç Pleyistosen-Holosen İklim Kayıtlarının Döngüselliği, *66th Geological Congress of Turkey*, 1-5 April, Ankara, Jeoloji Mühendisleri Odası Yayınları, 176-177.

Akçer, S., Çağatay, M.N., Sakınç, M., Ön, Z.B. and Acar, D. (2013) İstanbul'da "Küçük Buz Çağı" ve "Ortaçağ Ilık Dönemi": Küçükçekmece Lagünü Çökel Kayıtları ile Tarihi Kayıtların Deneştirilmesi, *66th Geological Congress of Turkey*, 1-5 April, Ankara, Jeoloji Mühendisleri Odası Yayınları, 164-165.